1991

Semiconductor quantum well and quantum wire lasers

Huzan Tanksalwalla
San Jose State University

Order Number 1347183

Semiconductor quantum well and quantum wire lasers

Tanksalwalla, Huzan, M.S.

San Jose State University, 1991

U·M·I
300 N. Zeeb Rd.
Ann Arbor, MI 48106

SEMICONDUCTOR QUANTUM WELL AND QUANTUM WIRE LASERS

A Thesis

presented to

The Faculty of the Department of Physics

San Jose State University

In Partial Fulfillment

of

the Requirements for the Degree of

Master of Science

by

Huzan Tanksalwalla

December, 1991

APPROVED FOR THE DEPARTMENT OF PHYSICS

Dr. Karamjeet Arya

Dr. H. Sarma Lakkaraju

Dr. Joseph F. Becker

APPROVED FOR THE UNIVERSITY

ABSTRACT

SEMICONDUCTOR QUANTUM WELL AND QUANTUM WIRE LASERS

by

Huzan Tanksalwalla

Semiconductor quantum well and quantum wire lasers have gained considerable attention in the past few years. Through quantum confinement of charge carriers and optical modes in the active region, these lasers show greatly enhanced optical gain and reduced operating threshold currents.

This thesis embodies theoretical studies of the optical gain in quasi-two- and quasi-one-dimensional GaAs/GaAlAs quantum well structures. Calculations of the gain coefficient are carried out for each case in two models, one using momentum conservation for optical transitions (k-selection rule) and the other not using momentum conservation (no k-selection rule).

Our studies show that optical gain increases by reducing the dimensions (from 3D to quasi-2D, to quasi-1D) of the active region. We have obtained the threshold current and temperature dependence of the optical gain in these lasers.

To my mother and father

Acknowledgements

I wish to thank Dr. K. Arya for his valuable guidance with my thesis, and Dr. S. Lakkaraju and Dr. J. Becker for their help and much appreciated suggestions. I also wish to thank Dr. Garcia for his help.

I am very grateful to my husband Anil for his patience, encouragement and understanding throughout my program. To my parents and family, I could never thank them enough for their love and unfailing support in all my endeavours.

TABLE OF CONTENTS

CHAPTER 1: INTRODUCTION

Theoretically proposed by A.L. Schawlow and C.H. Townes[1] in 1958, the laser was first successfully operated in 1960 by T.H. Maiman[2] (a flashlamp-pumped ruby laser at 694nm). Since then, laser technology has advanced in giant leaps, striving towards higher efficiency and adaptability. Solid state, gas, chemical, dye, and semiconductor lasers are individually important in various applications. However, economically and by the degree of its applications, the last kind has greater importance. Further, among semiconductor lasers, quantum well lasers are the most recent and most important discovery. The following sections include an overview of semiconductor lasers, and general description, uses, and importance of quantum well lasers.

1.1 Semiconductor Lasers

Simultaneously invented in 1961 by three separate research groups[3-5], semiconductor lasers were the first to step beyond specialized applications and the research field to mass consumers. This is attributed to their prime distinguishing features:

- Small physical size (typically[6] 200μm x 50μm x 10μm)
- Direct low power current pumping mechanism across the junction (typically[6] 15mA at 2V)

- The ability to modulate its output by direct modulation of the pumping current (at rates[6] exceeding 10GHz).
- Higher efficiency[6] (~ 40% to 50%) as compared to:
  gas lasers (HeNe, Ar^+ ~ 0.02%[7]; CO_2 ~ 27%[8], Excimer ~ 10%[8]),
  solid state lasers (Ruby ~ 0.01%[6], Nd:YAG < 5%[8]).
- Complex electronic energy level system because of a band structure. The numerous bands allow many more transitions, hence gain is larger.
- Low and "soft" threshold due to its high gain, strong spontaneous emission, broad linewidth and wide axial mode spacing (about[9] 10^{11}Hz≡10Å due to very small cavity volume). The smaller than average mode density (mode number~10^5-10^6) allows near-threshold operation (as opposed to "sharp" threshold lasers, which require extraordinary stability near threshold).

These same properties are shared by quantum well lasers. However, in the latter, the threshold is much lower and less temperature-dependent, and gain and efficiency can be much higher.

1.2 Quantum Well Lasers

Quantum well (QW) lasers are the most important class of semiconductor diode lasers[10,11]. Based on III-V semiconductors (and recently II-VI semiconductors[12]), the laser structure induces quantum size effects in the charge carriers through confinement in one, two or three dimensions.

Accordingly, the laser structure is quasi-two-dimensional, quasi-one dimensional, or quasi-zero-dimensional. (Henceforth, we shall assume the "quasi-" to be understood). The quantum confinement creates a dielectric waveguiding effect in the active region of the laser, which tightly confines optical radiation and concentrates modal energy in the region. The results are a much higher differential optical gain, lower threshold current and larger efficiency than those of a conventional diode laser.

The two most popular QW laser systems comprise of a GaAs layer "sandwiched" between (i) $Ga_{1-x}Al_xAs$ cladding layers, and (ii) $Ga_{1-x}In_xAs_{1-y}P_y$ cladding layers. The following sections expound on the description and uses of a GaAs/$Ga_{1-x}Al_xAs$ laser system.

1.2.1 Description of Two-dimensional QW Lasers

The basic unit of a two-dimensional (2D) QW laser is a double hetero-junction (DH junction), as depicted in Figure 1-1. A conventional DH junction consists of a thin active layer of semiconductor material (GaAs) sandwiched between oppositely doped cladding layers of higher band gap energy ($Ga_{1-x}Al_xAs$). The subscript x indicates the molar fraction of Ga molecules replaced by Al, and controls the band gap energy E_{g2} of $Ga_{1-x}Al_xAs$. The entire structure is stable (the lattice spacing is not disturbed) below a certain value of x. To ensure crystallographic continuity, the basic layered structure is grown epitaxially on a GaAs substrate.

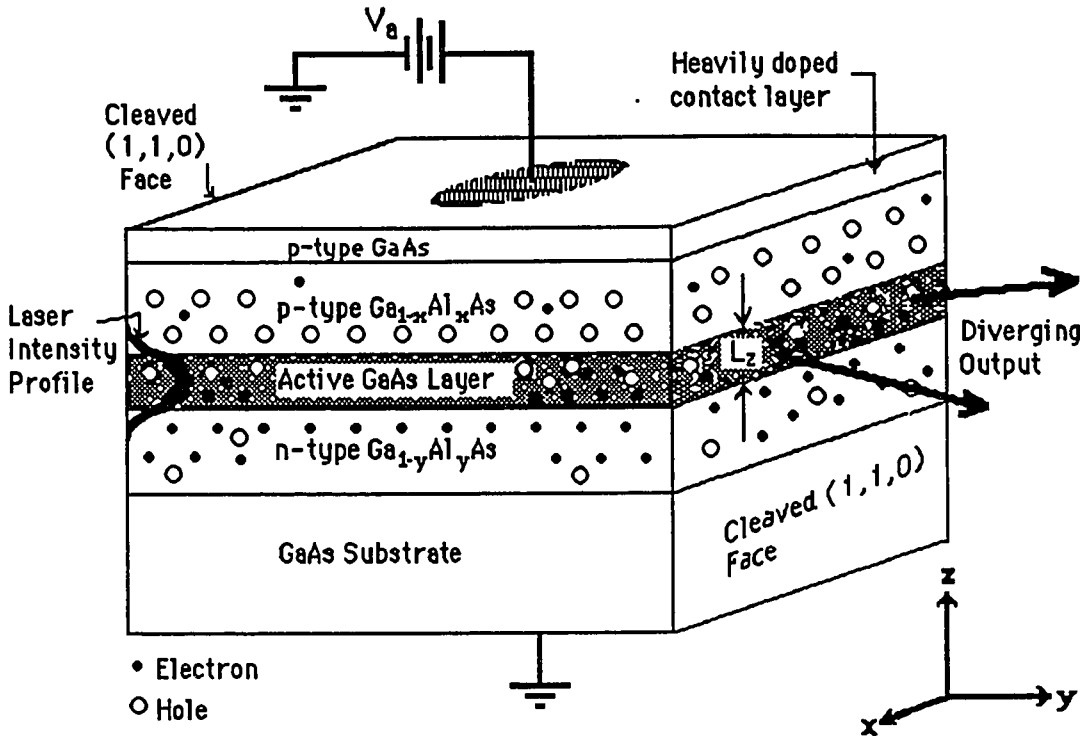

Figure 1-1: A typical double-heterostructure of a GaAs/$Ga_{1-x}Al_xAs$ two-dimensional QW laser.

Under forward bias, the above structure forms a potential well in the active region of height ΔE_c for electrons, which spatially coincides with a potential well of height ΔE_v for holes (see Figure 1-2(a) on the following page). For $x < 0.42$, E_{g2} can be approximated by[13]

$$E_{g2} = (1.424 + 1.266x)\ \text{eV}$$

where the bulk band gap energy E_{g1} of GaAs is 1.424 eV.

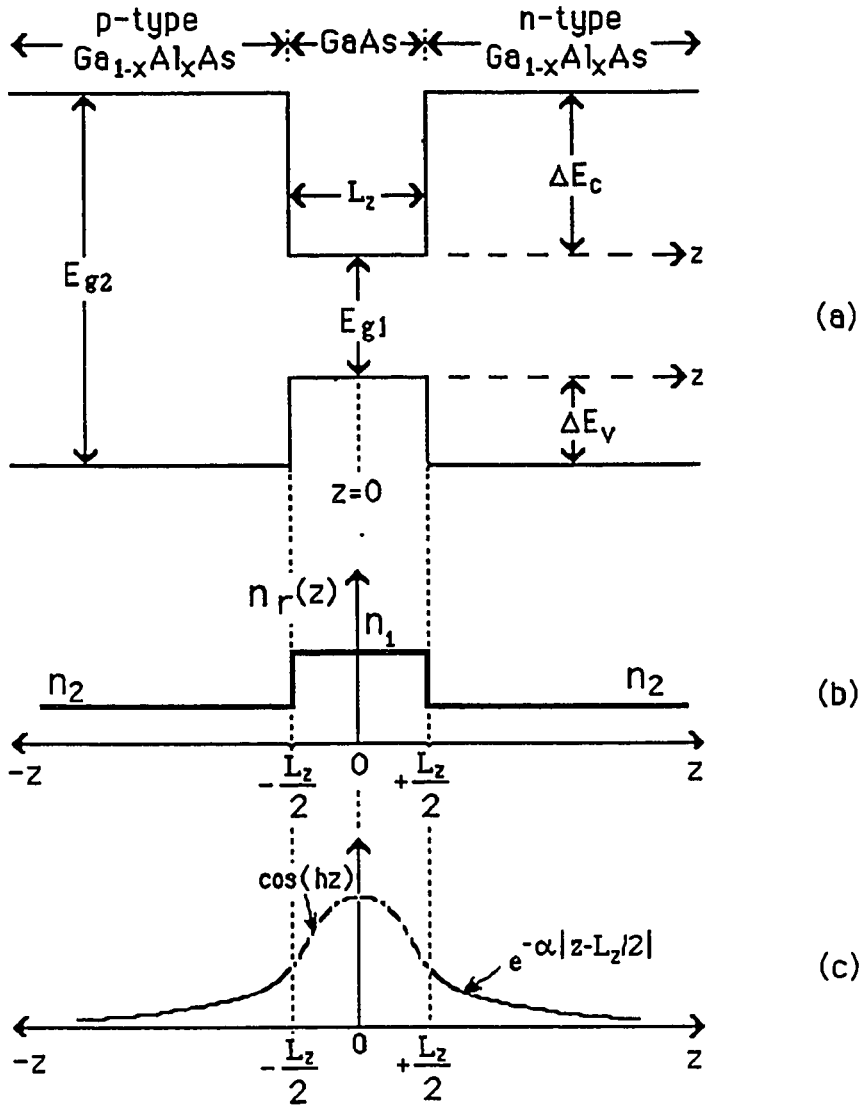

Figure 1-2: (a) Conduction band edges under a large positive forward bias, (b) the index of refraction profile, and (c) optical field (fundamental mode) of a GaAs/$Ga_{1-x}Al_xAs$ two-dimensional laser diode.

The total gap change $\Delta E_g \sim 1.266x$ eV is "divided" between conduction and valence bands as[13]

$$\Delta E_c \approx 0.67 \Delta E_{g2}$$
$$\Delta E_v \approx 0.33 \Delta E_{g2}$$

When the bias $eV_a \approx E_{g2}$, large densities of injected electrons from the n-type $Ga_{1-x}Al_xAs$ and holes from the p-type $Ga_{1-x}Al_xAs$ are trapped in the potential wells. This satisfies the inversion condition in the active region, and incoming radiation ω meeting the gain condition is amplified here.

The Al molar fraction also causes a lowering of the refractive index of the ternary $Ga_{1-x}Al_xAs$ crystal according to[6]

$$n_{GaAs} - n_{Ga_{1-x}Al_xAs} = n_1 - n_2 \approx 0.62x$$

This creates a three-layered dielectric waveguide, which confines the fundamental (lowest order) optical mode to the higher index region, *viz* GaAs. Since optical intensity in the guided mode varies inversely as the width of the waveguide for a fixed total power, the stimulated emission (and hence gain) scales inversely as the width of the active region. Figures 1-2(b) and (c) depict the index variation and a typical optical field distribution along the z-axis for the fundamental mode[13]. Within the active region, the field varies as a cosine function, while outside the region, it decays exponentially into the cladding layers.

We see that QW structures exhibit a double confinement of injected carriers and optical mode energy. This is the most important factor responsible for lower threshold and higher gain.

Other structures include growing a number of quantum wells in stacked fashion to increase the maximum gain and decrease divergence of the emergent beam[11]. Depending on the number of DH junctions present, the laser is termed a single or multiple quantum well laser.

1.2.2 Description of One-dimensional QW Lasers

The one-dimensional (1D) QW laser structure (also called Quantum Wire laser) is similar to the 2D QW laser with an additional confinement in a second orthogonal direction {refer to Figure 1-3}.

The laser forms potential wells as in Figure 1-2(a) along two perpendicular directions (y and z), and the injected carriers and optical mode are constrained to one dimensional motion. The band gap energies are controlled by the molar fractions x, y, and z, as before. The refractive index variation and modal intensity plots along the two chosen confining directions are similar to those depicted in Figures 1-2(b) and 1-2(c).

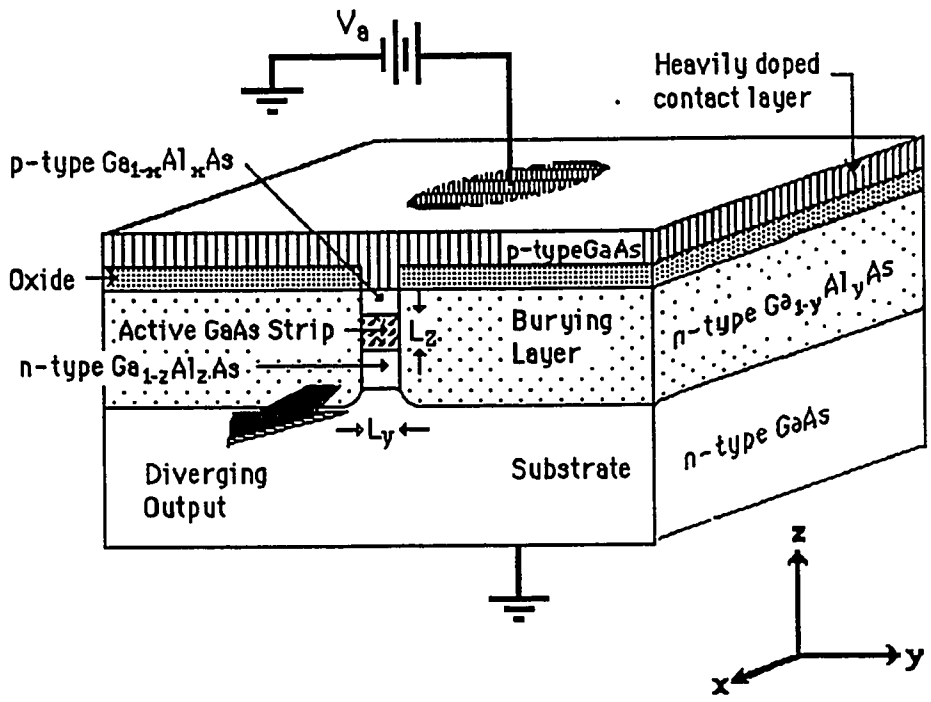

Figure 1-3: A typical buried-heterostructure of a GaAs/$Ga_{1-x}Al_xAs$ one-dimensional QW laser.

Here, simulated emission (and hence gain) scales as the cross-sectional area L_yL_z of the active region.

1.3 Usefulness of QW Lasers

QW lasers are naturally compatible with electronic circuitry, and allow monolithic integration. Their broad axial mode spacing[12] and ultrafast modulation properties[13-18] make them very important devices for optical communication and optical computers.

The uniqueness of QW lasers lies in the significant thinning of the active region (factor > 10). Compared to conventional semiconductor diode lasers, the total number of carriers required to achieve transparency decreases roughly by the ratio of the active region thicknesses. The free carrier absorption coefficient (modal), proportional to the number of carriers per unit area, is also reduced by the same factor. The net effect is a greatly enhanced gain[18], and a much reduced threshold current[13,15,16,18], which is also less temperature dependent[16,19-23]. In the following chapters, we expand on 2D and 1D QW lasers.

Chapter 2 covers derivations of the electronic states in quasi-2D and quasi-1D laser systems, which are necessary for obtaining the respective gain expressions. We shall explain the physical reason for increased gain and reduced temperature dependance with greater confinement in terms of the densities of states.

In Chapter 3, we obtain expressions for the gain coefficients in 2D and 1D QW laser systems in which momentum and energy are conserved. Graphs of the gain coefficient with varying parameters such as well width, temperature, and carrier concentration describe the gain behavior. We also compare the 2D and 1D gain coefficients with the bulk gain coefficient.

Chapter 4 comprises of derivations similar to those in Chapter 3 for systems in which momentum is not conserved, but total energy is. Similar graphs here with their interpretations further describe gain behavior.

In Chapter 5, we include a summary of the previous chapters, and further relevant discussion to bring out the advantages of moving towards reduced dimensions and working lasers in the quantum regime.

CHAPTER 2: ELECTRONIC STATES IN QUASI-TWO AND QUASI-ONE DIMENSIONAL SYSTEMS

In order to determine the optical gain in QW structures, we first require expressions for the electronic eigen energies and states. These are derived for both quasi-two and quasi-one dimensional quantum wells in the following sections, along with the density of states in each case. A comparison is then made between lower-dimensional densities of state with the bulk density of states.

2.1 Quantum Theory applied to the 2D Quantum Well

Consider a $GaAs/Ga_{1-x}Al_xAs$ "sandwich" similar to the one in Figure 1-2(a), with the interfaces lying in the xy-plane. Electrons in the conduction band (CB) and holes in the valence band (VB) are treated as free carriers with effective masses equal to those in the bulk material. Here, we derive results only for the electrons in the CB, as similar results may be directly obtained for holes in the VB. Henceforth, we shall denote the bulk band gap energy E_{g1} of GaAs as E_g.

2.1.1 Energy Eigenvalues and Wavefunctions

We assume electron motion along the x- and y- directions to be free (therefore under the influence of a constant potential assumed zero). Along

the z-direction, *i.e.* normal to the interfaces, the electron is bound in a potential well of height ΔE_c and width L_z. The Hamiltonian for the electron is written as

$$H_c(\mathbf{r}) = -\frac{\hbar^2}{2m_c}\nabla_{\|}^2 - \frac{\hbar^2}{2m_c}\nabla_z^2 + V_c(z) \qquad (2.1.1\text{-}1)$$

where the subscript 'c' denotes the conduction band, and $\nabla_{\|}^2 = \nabla_x^2 + \nabla_y^2$. The conduction band edge $V_c(z)$, *i.e.* the potential energy curve along the z-direction, is depicted in Figure 2-1 below.

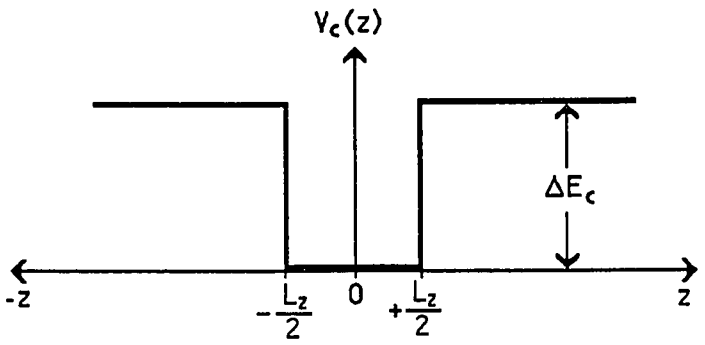

Figure 2-1: Conduction band edge along the z-direction of a single QW laser.

To obtain the energy eigenvalues and wavefunctions, we solve the following Schrödinger equation[13];

$$\left[-\frac{\hbar^2}{2m_c}\nabla_{\|}^2 - \frac{\hbar^2}{2m_c}\nabla_z^2 + V_c(z)\right]\Psi_c(\mathbf{r}_{\|},z) = E_c\,\Psi_c(\mathbf{r}_{\|},z) \qquad (2.1.1\text{-}2)$$

Using the "separation of variables" method, $\Psi_c(\mathbf{r}_{\|}, z)$ is written as[6]:

$$\Psi_c(\mathbf{r}_{\|}, z) = \psi_{k_{\|}}(\mathbf{r}_{\|})\, Z_c(z) \tag{2.1.1-3}$$

where $Z_c(z)$ satisfies the following equation;

$$\left[-\frac{\hbar^2}{2m_c}\nabla_z^2 + V_c(z) \right] Z_c(z) = \lambda_c Z_c(z) \tag{2.1.1-4}$$

and substituting (2.1.1-4) into (2.1.1-2), $\psi_{k_{\|}}(\mathbf{r}_{\|})$ satisfies

$$-\frac{\hbar^2}{2m_c}\nabla_{\|}^2 \psi_{k_{\|}}(\mathbf{r}_{\|}) = (E_c - \lambda_c)\, \psi_{k_{\|}}(\mathbf{r}_{\|}) \tag{2.1.1-5}$$

λ_c denotes the electron eigenvalues along the z-direction. The solution $\psi_{k_{\|}}(\mathbf{r}_{\|})$ of (2.1.1-5) describes plane wave motion of the electron in the xy-plane, *i.e.*

$$\psi_{k_{\|}}(\mathbf{r}_{\|}) = e^{i\mathbf{k}_{\|} \cdot \mathbf{r}_{\|}} \tag{2.1.1-6}$$

and the corresponding energy eigenvalues are given by

$$E_c = \lambda_c + \frac{\hbar^2}{2m_c} k_{\|}^2 \tag{2.1.1-7}$$

However, due to the crystalline nature of the medium, the electron is actually under the influence of a periodic potential along the xy-plane. We therefore consider $\psi_{k_{||}}(r_{||})$ to be a normalized Bloch state given by

$$\psi_{k_{||}}(r_{||}) = \frac{1}{\sqrt{N_u}} u_{k_{||}}(r_{||}) e^{i k_{||} \cdot r_{||}} \qquad (2.1.1\text{-}8)$$

where $u_{k_{||}}(r_{||})$ determines the periodicity of the wavefunction, and N_u is the normalization constant.

Now, QW lasers are usually operated near threshold frequencies. Thus, at low carrier concentrations, charge carriers in the active region occupy only the lowest energy levels. In this situation, the height of the well ΔE_c ($\approx$0.35eV) is much larger than the electron energy, and so may be approximated to infinity. We may then solve (2.1.1-4) simply as the problem of an infinite potential well, with the following boundary conditions,

$V_c(z) = 0$ for $-L_z/2 \le z \le L_z/2$

$V_c(z) \Rightarrow \infty$ for $z > L_z/2$ or $z < -L_z/2$

The normalized solutions and eigenvalues of (2.1.1-4) for $-L_z/2 \le z \le L_z/2$ are as follows:

$$Z_c(z) = \begin{cases} \sqrt{\frac{2}{L_z}} \cos\left(\frac{n\pi}{L_z} z\right) & \text{for } n = \text{even integer} \\ \sqrt{\frac{2}{L_z}} \sin\left(\frac{n\pi}{L_z} z\right) & \text{for } n = \text{odd integer} \end{cases} \tag{2.1.1-9}$$

$$\lambda_c \equiv E_{cn} = n^2 \frac{\hbar^2 \pi^2}{2m_c L_z^2} \quad ; \quad n = 1, 2, 3, \ldots\ldots \tag{2.1.1-10}$$

and $Z_c(z)$ is zero otherwise.

We may now write the complete normalized electron wavefunctions from (2.1.1-8 and -9), and eigenvalues from (2.1.1-7 and -10) as

$$\Psi_{Ck_{||}n}(\mathbf{r}_{||}, z) = \sqrt{\frac{2}{L_z}}\, \psi_{ck_{||}}(\mathbf{r}_{||})\, CS\left(\frac{n\pi}{L_z} z\right) \tag{2.1.1-11a}$$

$$E_c(\mathbf{k}_{||}, n) \equiv E_{Ck_{||}n} = \frac{\hbar^2 k_{||}^2}{2m_c} + \frac{\hbar^2 \pi^2}{2m_c} \frac{n^2}{L_z^2} \tag{2.1.1-12a}$$

where CS(x) denotes cos(x) or sin(x) according to whether n is an odd or even integer. Figure 2-2 shows the first few energy levels for an electron in the CB. Note that there now exists a non-zero positive minimum energy (zero-point energy) $E_{r1} = \hbar^2\pi^2/2m_cL_z^2$ due to quantization. Hence, the band gap energy in the 2D QW has effectively increased.

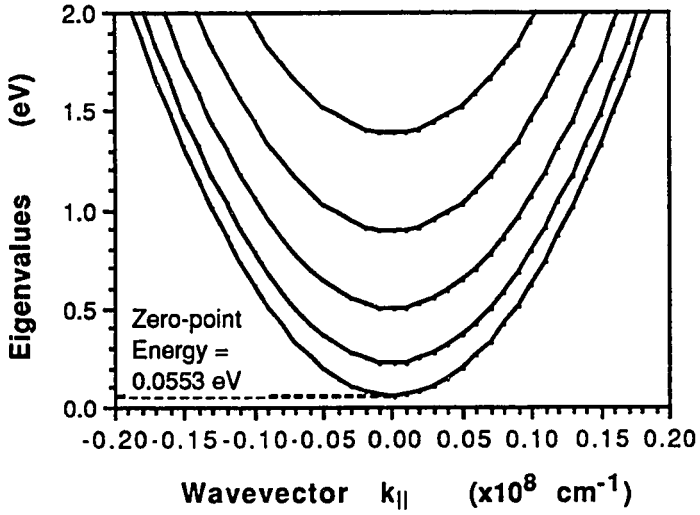

Figure 2-2: Electronic energy levels in the conduction band of a GaAs/$Ga_{1-x}Al_xAs$ double heterojunction.

Similar results apply to the holes in the valence band by replacing m_c by m_v. Hence, the complete normalized wavefunctions and eigenvalues for holes are

$$\Psi_{Vk_{||}n}(\mathbf{r}_{||}, z) = \sqrt{\frac{2}{L_z}}\,\psi_{vk_{||}}(\mathbf{r}_{||})\,CS\left(\frac{n\pi}{L_z}z\right) \qquad (2.1.1\text{-}11b)$$

$$E_v(k_{||}, n) \equiv E_{Vk_{||}n} = -\frac{\hbar^2 k_{||}^{\,2}}{2m_v} - \frac{\hbar^2\pi^2}{2m_v}\frac{n^2}{L_z^2} - E_g \qquad (2.1.1\text{-}12b)$$

where all energies are measured positive upwards and from the bottom of the single bulk CB in the chosen electronic energy diagrams. We have thus added '$-E_g$.' to the hole energies.

2.1.2 Density of States

According to Pauli's exclusion principle, since electrons are fermions, a maximum of two electrons (of opposite spin) may occupy the same energy state. Consider a conduction band similar to one of the bands in Figure 2-2. The total number of electrons N_{2D} filling all states up to an energy level $E_{Ck_{||}n}$ may be written as

$$N_{2D} = 2 \sum_{k_{||}, n} f(E_{Ck_{||}n}) \qquad (2.1.2\text{-}1)$$

where $f(E_{Ck_{||}n})$ is the Fermi-function for the electron in the CB.

The density of states is defined as the number of states per unit volume per unit energy. We may therefore write

$$N_{2D} = V \int dE\, \rho_{2D}(E)\, f(E) \qquad (2.1.2\text{-}2)$$

where V is the total volume. Comparing (2.1.2-1) and 2.1.2-2), we find that

$$\rho_{2D}(E) = \frac{2}{V} \sum_{k_{||}, n} \delta(E - E_{Ck_{||}n}) \qquad (2.1.2\text{-}3)$$

The expression for density of states is determined by changing the $k_{||}$ summation to an integration as follows;

$$\sum_{k_{||}} \rightarrow A_{||} \iint \frac{d^2k_{||}}{(2\pi)^2}$$

where $A_{||}$ is the area element in the xy-plane. Substituting the above into (2.1.2-3), we have

$$\rho_{2D}(E) = \frac{2}{L_z} \sum_{n=1}^{\infty} \iint \frac{d^2k_{||}}{(2\pi)^2} \delta (E - E_{Ck_{||}n}) \qquad (2.1.2\text{-}4)$$

where $V = L_z A_{||}$. We assume azimuthal symmetry to change the double integral $d^2k_{||}$ to the single integral $2\pi k_{||} dk_{||}$. Solving (2.1.1-12a) for $k_{||}$ and substituting this value into (2.1.2-4), the integration variable is changed to $E_{Ck_{||}n}$. The expression in (2.1.2-4) now changes to

$$\rho_{2D}(E) = \frac{1}{L_z} \frac{m_c}{\pi \hbar^2} \int_{E_{cn}}^{\infty} dE_{Ck_{||}n} \delta (E - E_{Ck_{||}n}) \qquad (2.1.2\text{-}5)$$

where we used the energy δ-function to set the limits of the integral, and E_{cn} is given in (2.1.1-10). Performing the integration, we obtain the quasi-2D density of states per unit volume $\rho_{2D}(E)$ as

$$\rho_{2D}(E) = \frac{1}{L_z}\frac{m_c}{\pi\hbar^2}\sum_{n=1}^{\infty} H\left[E - E_{cn}\right] \qquad (2.1.2\text{-}6)$$

where H[x] is the Heaviside step function, equal to one when $x \geq 0$ and zero when $x < 0$.

Figure 2-3 below depicts a plot of the volumetric density of states $\rho_{2D}(E)$ versus electron energy E. The dotted curve represents the bulk density of states $\rho_{3D}(E)$ in a conventional semiconductor medium.

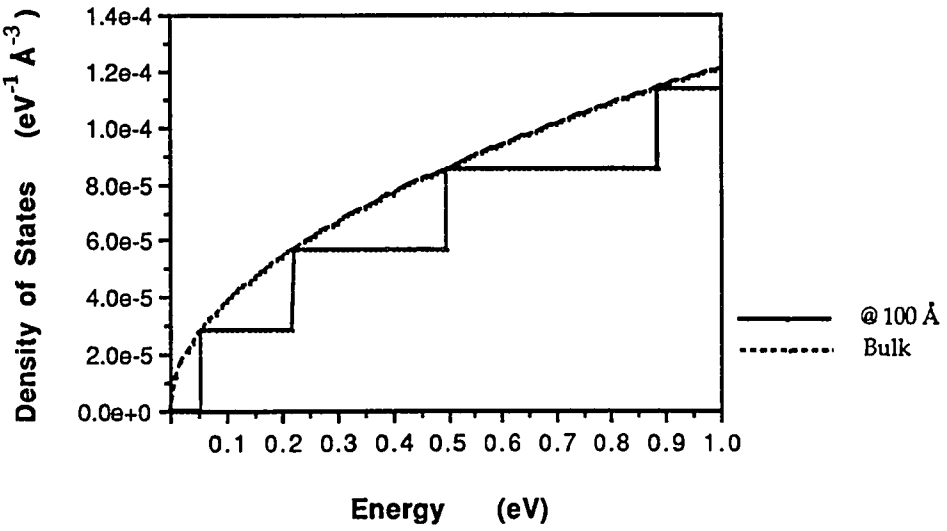

Figure 2-3: Volumetric two-dimensional density of states and bulk density of states plotted versus electron energy.

We observe that the QW density of states plot is a "staircase" of gradually increasing step lengths, coinciding with the bulk value at each step edge.

2.2 Quantum Theory applied to the 1D Quantum Well

Consider a 1D QW laser similar to the one in Figure 1-3(a). The interfaces GaAs/$Ga_{1-x}Al_xAs$ and GaAs/$Ga_{1-y}Al_yAs$ lie in the xy-plane and zx-plane, respectively. The treatment given for the 1D case here is similar to the 2D one in Section 2.1. As mentioned earlier, we shall consider the electrons in the CB and holes in the VB as free carriers in the effective mass approximation.

2.2.1 Energy Eigenvalues and Wavefunctions

In the 1D system, a conduction band electron in the active region is free only along the x-direction. Along the y- and z- directions, it is trapped in potential wells of heights ΔE_{cy} and ΔE_{cz}, and widths L_y and L_z, respectively. For simplicity, we choose the molar fractions x and y of the cladding layers $Ga_{1-x}Al_xAs$ and $Ga_{1-y}Al_yAs$ to be equal. Thus, the potential energy curves along the y- and z-directions are the same, given by $V_c(y,z)$, and $\Delta E_{cy} = \Delta E_{cz} = \Delta E_c$. The Hamiltonian for the electron is written as

$$H_c(\mathbf{r}) = -\frac{\hbar^2}{2m_c}\nabla_x^2 - \frac{\hbar^2}{2m_c}\nabla_y^2 - \frac{\hbar^2}{2m_c}\nabla_z^2 + V_c(y,z) \qquad (2.2.1\text{-}1)$$

where the subscript 'c' denotes the conduction band. The CB edge along the z-direction is identical to that depicted in Figure 2-1, with V(z) replaced by V(y,z). Along the y-direction, we get a similar picture by substituting y for z.

We solve the following Schrödinger equation to obtain the energy eigenvalues and wavefunctions;

$$\left[-\frac{\hbar^2}{2m_c}\nabla_x^2 - \frac{\hbar^2}{2m_c}\nabla_y^2 - \frac{\hbar^2}{2m_c}\nabla_z^2 + V_c(y,z)\right]\Psi_c(x,y,z) = E_c\Psi_c(x,y,z) \tag{2.2.1-2}$$

Separating the variables in $\Psi_c(x,y,z)$ as

$$\Psi_c(x,y,z) = \psi_{k_x}(x)Y_c(y)Z_c(z) \tag{2.2.1-3}$$

where $Y_c(y)$, $Z_c(z)$ and $\psi_{k_x}(x)$ satisfy the following;

$$\left[-\frac{\hbar^2}{2m_c}\nabla_y^2 - \frac{\hbar^2}{2m_c}\nabla_y^2 + V_c(y,z)\right]Y_c(y)Z_c(z) = \alpha_c Y_c(y)Z_c(z) \tag{2.2.1-4}$$

and

$$-\frac{\hbar^2}{2m_c}\nabla_x^2\,\psi_{k_x}(x) = \left[E_c - \alpha_c\right]\psi_{k_x}(x) \tag{2.2.1-5}$$

The solution $\psi_{k_x}(x)$ of (2.2.1-5) describes plane wave motion of the electron in the xy-plane, and may be written as

$$\psi_{k_x}(x) = e^{ik_x x} \tag{2.2.1-6}$$

The corresponding energy eigenvalues of (2.2.1-2) are thus

$$E_c = \alpha_c + \frac{\hbar^2}{2m_c} k_x^2 \tag{2.2.1-7}$$

Using the same argument of the crystalline nature of the medium, $\psi_{k_x}(x)$ is written as a normalized one-dimensional Bloch wavefunction as

$$\psi_{k_x}(x) = \frac{1}{\sqrt{N_u}} u_{k_x}(x)\, e^{ik_x x} \tag{2.2.1-8}$$

with $u_{k_x}(x)$ possessing the 1D crystal periodicity.

Now, electronic motion in the yz-plane described by (2.2.1-4) is not separable for the general form of potential $V_c(y,z)$ defining well height. However, as argued in Section 2.1.1, the well heights ΔE_c are approximated to infinity. Equation (2.2.1-4) is then simply solved as two separate problems of an infinite 1D potential well along the y-direction and the z-direction[24]. We rewrite (2.1.1-4) as

$$\left[-\frac{\hbar^2}{2m_c}\nabla_y^2 + V_c \right] Y_c(y) = \alpha_{cy} Y_c(y) \tag{2.2.1-4a}$$

$$\left[-\frac{\hbar^2}{2m_c}\nabla_z^2 + V_c \right] Z_c(z) = \alpha_{cz} Z_c(z) \tag{2.2.1-4b}$$

where V_c is now a constant potential equal to zero in the well, and infinite outside it. Following similar steps to Section 2.1.1, the normalized solutions and eigenvalues of (2.2.1-4a) for $-L_y/2 \le y \le L_y/2$ are

$$Y_c(y) = \begin{cases} \sqrt{\frac{2}{L_y}} \cos\left(\frac{m\pi}{L_y} y\right) & \text{for } m = \text{even integer} \\ \sqrt{\frac{2}{L_y}} \sin\left(\frac{m\pi}{L_y} y\right) & \text{for } m = \text{odd integer} \end{cases} \qquad (2.2.1\text{-}9)$$

$$\alpha_{cy} \equiv E_{cm} = m^2 \frac{\hbar^2 \pi^2}{2 m_c L_y^2} \quad ; \quad m = 1, 2, 3, \ldots\ldots \qquad (2.2.1\text{-}10)$$

and $Y_c(y)$ is zero otherwise.

Similarly, the normalized solutions and eigenvalues of (2.2.1-4b) for $-L_z/2 \le z \le L_z/2$ are

$$Z_c(z) = \begin{cases} \sqrt{\frac{2}{L_z}} \cos\left(\frac{n\pi}{L_y} z\right) & \text{for } n = \text{even integer} \\ \sqrt{\frac{2}{L_z}} \sin\left(\frac{n\pi}{L_y} z\right) & \text{for } n = \text{odd integer} \end{cases} \qquad (2.2.1\text{-}11)$$

$$\alpha_{cz} \equiv E_{cn} = n^2 \frac{\hbar^2 \pi^2}{2 m_c L_z^2} \quad ; \quad n = 1, 2, 3, \ldots\ldots \qquad (2.2.1\text{-}12)$$

and $Z_c(z)$ is zero otherwise.

Finally, using (2.2.1-3,-8,-9,-11) and (2.2.1-7,-10,-12), we may write the complete normalized electron wavefunctions and energy eigenvalues as

$$\Psi_{Ck_x mn}(x, y, z) = \frac{2}{\sqrt{L_y L_z}} \psi_{k_x}(x)\, CS\left(\frac{m\pi}{L_y} y\right) CS\left(\frac{n\pi}{L_z} z\right) \qquad (2.2.1\text{-}13a)$$

$$E_c(k_x,m,n) \equiv E_{Ck_x mn} = \frac{\hbar^2 k_x^2}{2m_c} + \frac{\hbar^2\pi^2}{2m_c}\left[\frac{m^2}{L_y^2} + \frac{n^2}{L_z^2}\right] \qquad (2.2.1\text{-}14a)$$

where CS(x) denotes cos(x) or sin(x) according to whether m or n is odd or even. Figure 2-4 shows the first few energy levels (where m=n) for an electron in the CB. Once again, there exists a zero-point energy $E_{r11} = (\hbar^2\pi^2/2m_c)(L_y^{-2}+L_z^{-2})$ due to quantization. This effective increase in band gap energy in the 1D QW is larger than that in the 2D QW.

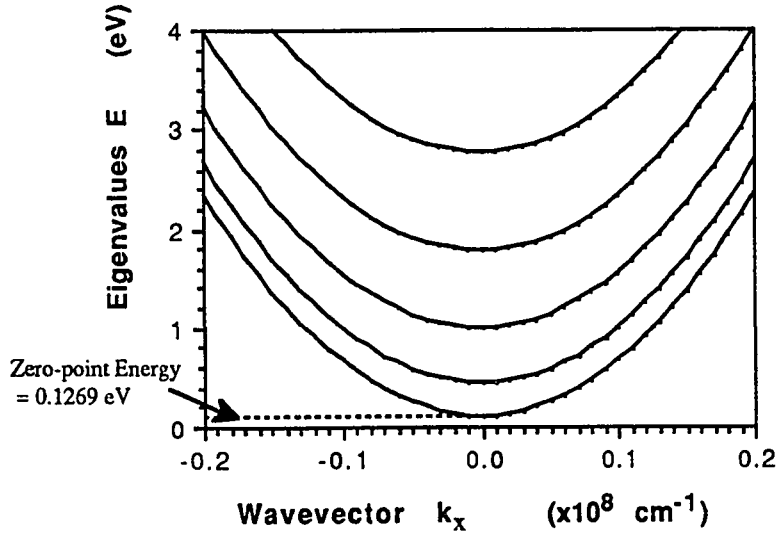

Figure 2-4: Electronic energy levels in the conduction band of a one-dimensional GaAs/$Ga_{1-x}Al_xAs$ double heterojunction.

By replacing m_c by m_v, similar results can be obtained for holes in the VB. Hence, the complete normalized wavefunctions and eigenvalues for holes are

$$\Psi_{Vk_x mn}(x, y, z) = \frac{2}{\sqrt{L_y L_z}} \psi_{k_x}(x)\, CS\left(\frac{m\pi}{L_y} y\right) CS\left(\frac{n\pi}{L_z} z\right) \qquad (2.2.1\text{-}13b)$$

$$E_v(k_x, m, n) \equiv E_{Vk_x mn} = -\frac{\hbar^2 k_x^2}{2m_v} - \frac{\hbar^2 \pi^2}{2m_v}\left[\frac{m^2}{L_y^2} + \frac{n^2}{L_z^2}\right] - E_g \qquad (2.2.1\text{-}14b)$$

where hole energies are measured positive upwards, and from the bottom of the single bulk CB.

2.2.2 Density of States

Derivation of the quasi-1D density of states follows a similar path as in Section 2.1.2. The expression for the general density of states from (2.1.2-3) is modified for the 1D case as

$$\rho_{1D}(E) = \frac{2}{V} \sum_{k_x,\, m,\, n} \delta\,(E - E_{Ck_x mn}) \qquad (2.2.2\text{-}1)$$

Once again, we change the k_x summation to an integration as

$$\sum_{k_x} \rightarrow L_x \int_{-\infty}^{\infty} \frac{dk_x}{2\pi} \equiv L_x \, 2 \int_{0}^{\infty} \frac{dk_x}{2\pi}$$

where L_x is the line element in the x-direction, and the even integrand allows changing of the limits as shown. Substituting the above into (2.2.2-1), we have

$$\rho_{1D}(E) = \frac{2}{L_y L_z} \sum_{m,\, n=1}^{\infty} 2 \int_{0}^{\infty} \frac{dk_x}{2\pi} \, \delta (E - E_{Ck_x mn}) \qquad (2.2.2\text{-}2)$$

where $V = L_x L_y L_z$. Solving (2.2.1-14a) for k_x and substituting this value into (2.2.2-2), we change the integration variable to $E_{Ck_x mn}$. The expression in (2.2.2-2) now changes to

$$\rho_{1D}(E) = \frac{1}{\pi L_y L_z} \sqrt{\frac{2m_c}{\hbar^2}} \int_{(E_{cm}+E_{cn})}^{\infty} dE_{Ck_x mn} \left[E_{Ck_x mn} - E_{cm} - E_{cn} \right]^{-1/2} \delta (E - E_{Ck_x mn}) \qquad (2.2.2\text{-}3)$$

where we used the energy δ-function to set the limits of the integral. E_{cm} and E_{cn} are given in (2.2.1-10) and (2.2.1-12), respectively. Performing the integration, we obtain the quasi-1D density of states per unit volume $\rho_{1D}(E)$ as

$$\rho_{1D}(E) = \frac{1}{\pi L_y L_z} \sqrt{\frac{2m_c}{\hbar^2}} \sum_{m,\, n=1}^{\infty} \left[E - E_{cm} - E_{cn} \right]^{-1/2} H \left[E - E_{cm} - E_{cn} \right] \qquad (2.2.2\text{-}4)$$

where H[x] is the Heaviside step function, as defined in section 2.1.2.

Figure 2-5 depicts a plot of the volumetric density of states $\rho_{1D}(E)$ versus electron energy E. For comparison, we have shown the bulk density of states in a conventional semiconductor medium as a broken curve. Theoretically, the peaks tend to infinity, but we have terminated them at a finite upper limit during calculation.

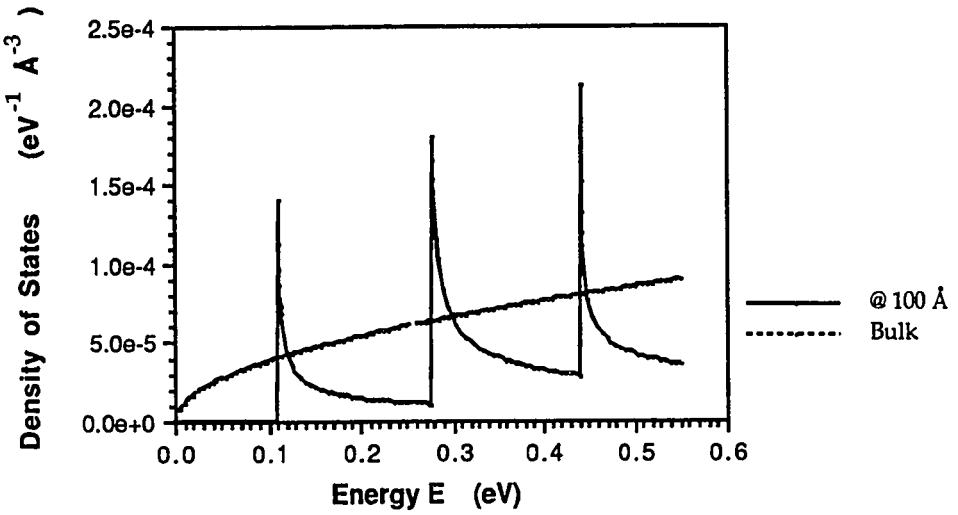

Figure 2-5: Volumetric one-dimensional density of states and bulk density of states plotted versus electron energy.

2.3 Comparison of 1D, 2D, and Bulk Densities of States

Looking at the plot of the 2D and bulk densities of states we note the following. The bulk or three-dimensional (3D) density of states has a minimum value of zero, while the 2D one starts at a constant positive value, inversely proportional to well width. Hence, we expect the threshold gain for a 2D QW laser to be much larger than that for a bulk diode laser. Similarly, the 1D density of states at threshold is much larger (theoretically infinite)

than either the 3D or the 2D density of states. This is an obvious reason for the optical gain in DH structure lasers to increase with increased confinement of charge carriers[17,25].

Secondly, the expression for the 2D (1D) density of states reduces to the 3D one in the relevant limiting case of L_z (L_y and L_z) tending to infinity. Physically, this simply implies that the quantum well structure has been reduced to a bulk structure. We demonstrate this fact for the 1D case in the following paragraphs.

Consider the expression for the 1D density of states given by (2.2.2-4). In the limiting case that L_y and L_z are very large, the quantum numbers m and n may be considered to be continuous rather than discrete values. The summations over m and n are thus replaced by integrals. From (2.2.2-4), we therefore have

$$\lim_{L_y, L_z \to \infty} \rho_{1D}(E) = \sqrt{\frac{2m_c}{\pi^2 \hbar^2}} \lim_{L_y, L_z \to \infty} \frac{1}{L_y L_z} \int_0^{\infty} \int_0^{\infty} \left[E - E_{cm} - E_{cn}\right]^{-1/2} \mathbf{H}\left[E - E_{cm} - E_{cn}\right] dm\, dn \tag{2.3-1}$$

where we have taken the integration limits as 0 to ∞, even though the summations go from 1 to ∞. This is a reasonable approximation, because the

significant contributions to the summation come only from very large m and n.

Using the step function to set the upper limit on the n-integration, we can obtain a non-zero integral only if

$$E_{cn} \leq E - E_{cm} \tag{2.3-2}$$

To perform the integrations, we change the variables m and n to E_{cm} and E_{cn}. Thus, from (2.2.1-10) and (2.2.1-12), we have

$$dm = \sqrt{\frac{m_c}{2\pi^2\hbar^2}}\, L_y\, E_{cm}^{-\frac{1}{2}}\, dE_{cm} \tag{2.3-3a}$$

$$dn = \sqrt{\frac{m_c}{2\pi^2\hbar^2}}\, L_z\, E_{cn}^{-\frac{1}{2}}\, dE_{cn} \tag{2.3-3b}$$

Substituting (2.3-2, -3a and -3b) into (2.3-1) and simplifying, we have

$$\lim_{L_y, L_z \to \infty} \rho_{1D}(E) = \sqrt{\frac{2m_c}{\pi^2\hbar^2}} \lim_{L_y, L_z \to \infty} \left(\frac{m_c}{2\pi^2\hbar^2}\right) \int_0^{\infty} dE_{cm}\, E_{cm}^{-\frac{1}{2}} \int_0^{E-E_{cm}} dE_{cn}\, (E - E_{cm} - E_{cn})^{-\frac{1}{2}}\, E_{cn}^{-\frac{1}{2}} \tag{2.3-4}$$

To perform the E_{cn}-integration now, we use a variable change as follows:

$$(E - E_{cm} - E_{cn})^{\frac{1}{2}} = t$$

and find that

$$\lim_{L_y, L_z \to \infty} \rho_{1D}(E) = \frac{\pi}{\sqrt{2}} \left(\frac{m_c}{\pi^2 \hbar^2} \right)^{\frac{3}{2}} \int_0^{\infty} dE_{cm} E_{cm}^{-\frac{1}{2}} H\left[E - E_{cm}\right]$$

where the step function is necessarily added to satisfy energy conservation. We perform the simple E_{cm}-integration, using the step function to limit the integration from 0 to $E\text{-}E_{cn}$, and obtain

$$\lim_{L_y, L_z \to \infty} \rho_{1D}(E) = \frac{1}{2\pi^2} \left(\frac{2m_c}{\hbar^2} \right)^{\frac{3}{2}} E^{\frac{1}{2}} \equiv \rho_{3D}(E)$$

i.e., in the limiting case of L_y and L_z tending to ∞, the 1D density of states reduces to the 3D expression. A similar proof for the 2D case can be easily derived.

The electronic states determined in this chapter are now used to calculate optical gain in QW laser systems where momentum is conserved (Chapter 3), and not conserved (Chapter 4).

CHAPTER 3: OPTICAL GAIN IN QW LASERS USING THE k-SELECTION RULE

To determine the optical gain of quantum well lasers, we need to calculate the probability of transition between the two lasing levels. Here, we first derive the transition probability for a laser system in general using time-dependent perturbation theory. Thereafter, we obtain expressions for probabilities in the particular cases of 2D and 1D QW lasers. Finally, we determine the optical gain in each case, and include a short comparison of the two situations with the 3D system.

3.1 Transition Probability

Consider a single electron moving in a potential V(r) in the active region of a semiconductor laser. We assume its motion is described by the unperturbed Hamiltonian as[26]

$$H_0 = \frac{p^2}{2m_c} + V(\mathbf{r}) \qquad (3.1\text{-}1)$$

The system is now perturbed by subjecting it to external electromagnetic (EM) radiation (*i.e.*, shining light on it). The new perturbed Hamiltonian is obtained by changing the momentum operator p to (p-eA/c), as below

$$H = \frac{1}{2m_c}\left(\mathbf{p} - \frac{e\mathbf{A}}{c}\right)^2 + V(\mathbf{r}) \qquad (3.1\text{-}2)$$

where **A** is the vector potential. In terms of **A**, the electric and magnetic fields in the Coulomb (transverse) gauge are written as[27]

$$\mathbf{E} = -\frac{1}{c}\frac{\partial \mathbf{A}}{\partial t}$$
$$\mathbf{B} = \nabla \times \mathbf{A}$$

and $\nabla \cdot \mathbf{A} = 0$. Assuming EM radiation of single frequency, we may write

$$\mathbf{A}(\mathbf{r}, t) = \mathbf{A}_0(\mathbf{q}, \omega)\, e^{i\mathbf{q}\cdot\mathbf{r}} e^{-i\omega t} + \text{complex conjugate} \qquad (3.1\text{-}3)$$

Equation (3.1-2) may be written as,

$$H = H_0 + H_A + H_{AA} \qquad (3.1\text{-}4)$$

where H_0 is the unperturbed Hamiltonian given by (3.1-1), H_A and H_{AA} are the first and second order terms in the vector potential **A**.

$$H_A = -\frac{e}{2m_c c}(\mathbf{p}\cdot\mathbf{A} + \mathbf{A}\cdot\mathbf{p}) \qquad (3.1\text{-}5)$$

$$H_{AA} = \frac{e^2}{2m_c c^2}A^2 \qquad (3.1\text{-}6)$$

For the assumed transverse EM field (as is the case for most laser experiments), the first order perturbation H_A in (3.1-5) simplifies to

$$H_A = - \frac{e}{m_c c} (\mathbf{A} \bullet \mathbf{p}) \qquad (3.1\text{-}7)$$

The transition probability W_{if} between an initial state Ψ_i and a final state Ψ_f due to the EM interaction (H_A+H_{AA}) is given by *Fermi's Golden Rule* as[28],

$$W_{if} = \frac{2\pi}{\hbar} \left| \langle \Psi_f | (H_A + H_{AA}) | \Psi_i \rangle \right|^2 \delta (E_f - E_i + \hbar\omega) \qquad (3.1\text{-}8)$$

where the δ-function on the right hand side implies energy conservation.

In order to calculate the optical gain, it suffices to consider only first order perturbation H_A in (3.1-8). However, it is necessary to include the H_{AA} term when discussing finer effects such as scattering, two-photon absorption and emission, stimulated phonon emission[29], non-linear effects[30], and so on. Hence, substituting for H_A from (3.1-7) in (3.1-8),

$$W_{if} = \frac{2\pi}{\hbar} \left| \left\langle \Psi_f \left| -\frac{e}{m_c c} \mathbf{A}(\mathbf{r}, \omega) \bullet \mathbf{p} \right| \Psi_i \right\rangle \right|^2 \delta (E_f - E_i + \hbar\omega) \qquad (3.1\text{-}9)$$

where,

$$\mathbf{A}(\mathbf{r}, \omega) = A_0(\mathbf{q}, \omega)\, e^{i\mathbf{q}\bullet\mathbf{r}} \qquad (3.1\text{-}10)$$

Thus, replacing the above expression for **A** in (3.1-9), we have

$$W_{if} = \frac{2\pi e^2}{\hbar m_c^2 c^2} \left| \left\langle \Psi_f \left| e^{iq\bullet r} A_0 \bullet p \right| \Psi_i \right\rangle \right|^2 \delta (E_f - E_i + \hbar\omega) \qquad (3.1\text{-}11)$$

The total transition probability per unit time for all possible electronic transitions induced by light of frequency ω is obtained by summing over all occupied initial and unoccupied final states. In semiconductor (thus QW) lasers, all electronic transitions between the CB and VB are considered. Now, transitions from the CB to VB correspond to the emission of photons, while those from the VB to CB correspond to the absorption of photons. Thus, the transition probability W for the net photon emission is written as

$$W = \frac{2\pi e^2}{\hbar m_c^2 c^2} \sum_i \sum_f \left| \left\langle \Psi_f \left| e^{iq\bullet r} A_0 \bullet p \right| \Psi_i \right\rangle \right|^2 \left[f_c(E_i) - f_v(E_f) \right] \delta (E_f - E_i + \hbar\omega) \qquad (3.1\text{-}12)$$

where $f_c(E)$ and $f_v(E)$ denote the Fermi functions for the electron in the CB and VB, respectively. They are given by[31]

$$f_c(E) = \frac{1}{e^{(E - E_{fc})/kT} + 1} \qquad (3.1\text{-}13a)$$

$$f_v(E) = \frac{1}{e^{(E - E_{fv})/kT} + 1} \qquad (3.1\text{-}13b)$$

where E_{fc} and E_{fv} are the quasi-Fermi energies at a non-zero temperature T for electrons in the CB and VB, respectively. If the Fermi energies $E_{fc}(0)$ and $E_{fv}(0)$ at T=0 are less than or equal to kT, then the Fermi energies $E_{fc}(T)$ and $E_{fv}(T)$ at T>0 are equal to those at T=0. Otherwise[32],

$$E_{fc} = E_{fc}(T) = E_{fc}(0)\left[1 - \frac{\pi^2}{12}\left(\frac{kT}{E_{fc}(0)}\right)^2\right] \tag{3.1-14a}$$

$$E_{fv} = -E_{fv}(T) = -E_{fv}(0)\left[1 - \frac{\pi^2}{12}\left(\frac{kT}{E_{fv}(0)}\right)^2\right] - E_g \tag{3.1-14b}$$

where

$$E_{fc}(0) = \frac{\hbar^2}{2m_c}(3\pi^2 N_0)^{1/3} \tag{3.1-15a}$$

$$E_{fv}(0) = -\frac{\hbar^2}{2m_v}(3\pi^2 N_0)^{1/3} \tag{3.1-15b}$$

Note that all energies are measured as before. The following sub-sections present explicit calculations for transition probabilities in the 2D and 1D QW lasers.

3.1.1 Transition Probability in a 2D QW laser

The initial and final states of an electron undergoing a transition are represented by any single conduction band and valence band, respectively, in the active region of a 2D QW laser. From (2.1.1-8) and (2.1.1-11a,b) in Chapter 2, we rewrite the relevant electronic wavefunctions as

$$\Psi_i = \Psi_{Ck_{\|}n}(r_{\|}, z) = \sqrt{\frac{2}{L_z N_u}}\, u_{Ck_{\|}}(r_{\|}) e^{ik_{\|}\bullet r_{\|}} CS\left(\frac{n\pi}{L_z} z\right) \quad (3.1.1\text{-}1a)$$

$$\Psi_f = \Psi_{Vk'_{\|}n'}(r_{\|}, z) = \sqrt{\frac{2}{L_z N_u}}\, u_{Vk'_{\|}}(r_{\|}) e^{ik'_{\|}\bullet r_{\|}} CS\left(\frac{n'\pi}{L_z} z\right) \quad (3.1.1\text{-}1b)$$

These wavefunctions are substituted into (3.1-12) to solve the matrix element $(M_{if})_{2D}$ for the 2D case. Thus, we have

$$(M_{if})_{2D} = \left\langle \Psi_{Vk'_{\|}n'} \middle| e^{iq\bullet r} A_0 \bullet p \middle| \Psi_{Ck_{\|}n} \right\rangle$$

$$= \frac{2}{L_z N_u} \iiint u^*_{Vk'_{\|}}(r_{\|}) e^{-ik'_{\|}\bullet r_{\|}} CS\left(\frac{n'\pi}{L_z} z\right) e^{iq\bullet r} A_0 \bullet p\, u_{Ck_{\|}}(r_{\|}) e^{ik_{\|}\bullet r_{\|}} CS\left(\frac{n\pi}{L_z} z\right) d^3r \quad (3.1.1\text{-}2)$$

Since the active region is a semiconductor crystal, it is comprised of identical unit cells in periodic array. We may therefore rewrite the 3D position vector r(x,y,z) of an arbitrary point (x,y,z) in the active region as[31]:

$$r(x,y,z) = r_{\|} + \hat{z}z = \{\rho_{\|} + R_{\|i}\} + \hat{z}z \quad (3.1.1\text{-}3)$$

where $R_{\|i}$ determines the position of the 2D unit cell, and $\rho_{\|}$ the displacement of the point relative to the 'address' $R_{\|i}$ of the unit cell. Since all unit cells are identical, the integral over the crystal may be expressed as an integral over any single unit cell summed over all unit cells. Substituting (3.1.1-3) into (3.1.1-2), we have

$$(M_{if})_{2D} = \frac{2}{L_z N_u} \sum_{i=1}^{N_u} \iiint u^*_{Vk'_{\|}}(\rho_{\|} + R_{\|i}) e^{-i k'_{\|} \bullet (\rho_{\|} + R_{\|i})} CS\left(\frac{n'\pi}{L_z} z\right)$$

$$e^{i q_{\|} \bullet (\rho_{\|} + R_{\|i})} e^{i q_z z} A_0 \bullet p\, u_{Ck_{\|}}(\rho_{\|} + R_{\|i}) e^{i k_{\|} \bullet (\rho_{\|} + R_{\|i})} CS\left(\frac{n\pi}{L_z} z\right) d^2\rho_{\|} dz \qquad (3.1.1\text{-}4)$$

Since the integral is now over $\rho_{\|}$, we may gather terms in $R_{\|i}$ outside the integral sign. We note that the summation

$$\sum_{i=1}^{N_u} e^{i(-k'_{\|} + q_{\|} + k_{\|}) \bullet R_{\|i}} = N_u\, \delta(-k'_{\|} + k_{\|} - q_{\|}) \qquad (3.1.1\text{-}5)$$

where $\delta(-k_{\|}' + k_{\|} + q_{\|})$ essentially ensures momentum conservation. Also, since the functions $u_{Ck_{\|}}$ and $u_{Vk'_{\|}}$ are periodic with the same periodicity as the crystal, therefore

$$u_{Ck_{\|}}(\rho_{\|} + R_{\|i}) = u_{Ck_{\|}}(\rho_{\|})$$
$$u_{Vk'_{\|}}(\rho_{\|} + R_{\|i}) = u_{Vk'_{\|}}(\rho_{\|})$$

Using the above expressions and (3.1.1-5) in (3.1.1-4), the matrix element expression thus simplifies to

$$(M_{if})_{2D} = \frac{2}{L_z}\delta(-k'_{\|}+k_{\|}+q_{\|}) \iiint_{\text{any unit cell}} u^{*}_{Vk'_{\|}}(\rho_{\|}) e^{-ik'_{\|}\cdot\rho_{\|}} CS\left(\frac{n'\pi}{L_z}z\right) e^{iq_{\|}\cdot\rho_{\|}} e^{iq_z z} A_0 \cdot p\, u_{Ck_{\|}}(\rho_{\|}) e^{ik_{\|}\cdot\rho_{\|}} CS\left(\frac{n\pi}{L_z}z\right) d^2\rho_{\|} dz \qquad (3.1.1\text{-}6)$$

Using the relation

$$p\, u_{Ck_{\|}}(\rho_{\|}) e^{ik_{\|}\cdot\rho_{\|}} CS\left(\frac{n\pi}{L_z}z\right) = e^{ik_{\|}\cdot\rho_{\|}} (\hbar k_{\|} + p)\, u_{Ck_{\|}}(\rho_{\|}) e^{ik_{\|}\cdot\rho_{\|}} CS\left(\frac{n\pi}{L_z}z\right)$$

and the momentum δ-function to allow $e^{i(-k'_{\|}+k_{\|}-q_{\|})} = 1$ in (3.1.1-6), we have

$$(M_{if})_{2D} = \frac{2}{L_z}\delta(-k'_{\|}+k_{\|}+q_{\|}) \iiint_{\text{any unit cell}} u^{*}_{Vk'_{\|}}(\rho_{\|}) CS\left(\frac{n'\pi}{L_z}z\right) e^{iq_z z} A_0 \cdot (\hbar k_{\|} + p) u_{Ck_{\|}}(\rho_{\|}) CS\left(\frac{n\pi}{L_z}z\right) d^2\rho_{\|} dz \qquad (3.1.1\text{-}7)$$

We recall that **q** represents the photon momentum and make the following argument. For typical photon energies in the visible range (~1 eV *i.e.* wavelengths ~ 10^4Å), $|q| \approx 2\pi/10^4$ Å^{-1}. The range of variation of k' (and k) is $2\pi/a$, lattice spacing a being of the order of a few Angstroms. Thus, for all practical purposes, **q** is negligible in magnitude compared to k' and k, and the momentum δ-function implies that the electron transits with k=k'. In other

words, only "vertical transitions" are induced by the electromagnetic radiation in the energy band diagram. This is sometimes referred to as the *k-Selection Rule.*[15,23]

Using this approximation (*i.e.* $e^{iq_z z} \approx 1$) along with the orthonormality of the Bloch functions, *i.e.* $\langle u_{Vk'_{||}} | k_{||} | u_{Ck_{||}} \rangle = 0$), equation (3.1.1-7) reduces to

$$(M_{if})_{2D} = \frac{2}{L_z}\delta(k_{||} - k'_{||}) \iiint_{\text{any unit cell}} u^*_{Vk'_{||}}(\rho_{||})\, CS\left(\frac{n'\pi}{L_z} z\right)\, A_0 \bullet p\, u_{Ck_{||}}(\rho_{||})\, CS\left(\frac{n\pi}{L_z} z\right) d^2\rho_{||} dz \qquad (3.1.1\text{-}8)$$

Further, we expand the momentum operator $\mathbf{p} = \mathbf{p}_{||} + \hat{\mathbf{z}} p_z$ as

$$p\, u_{Ck_{||}}(\rho_{||})\, CS\left(\frac{n\pi}{L_z} z\right) = CS\left(\frac{n\pi}{L_z} z\right) p_{||} u_{Ck_{||}}(\rho_{||}) + u_{Ck_{||}}(\rho_{||}) \left(\pm i\hbar \frac{n\pi}{L_z}\right) SC\left(\frac{n\pi}{L_z} z\right)$$

Substituting the above into (3.1.1-8), we note that the z-integration with respect to the second term goes to zero. We therefore obtain

$$(M_{if})_{2D} = \delta_{nn'}\, \delta(k_{||} - k'_{||})\, A_0 \bullet M_{CV}(k_{||}) \qquad (3.1.1\text{-}9)$$

where $M_{CV}(k_{||})$ is the matrix element given by

$$M_{CV}(k_{\|}) = \iint_{\substack{\text{any 2D} \\ \text{unit cell}}} u^{*}_{Vk_{\|}}(\rho_{\|})\, p_{\|}\, u_{Ck_{\|}}(\rho_{\|})\, d^2\rho_{\|} \qquad (3.1.1\text{-}10)$$

and the Kronecker delta function $\delta_{nn'}$ appears due to the orthonormality of the CS functions.

We now recall the expression for the total transition probability given by (3.1-12). The initial state summation implies a summation over $k_{\|}'$ and n', while the final state summation over $k_{\|}$ and n. Substituting (3.1.1-9) into (3.1-12), the summations over $k_{\|}'$ and n' with the respective δ-functions are performed. The total transition probability per unit time for the net emission of photons of frequency ω is given as

$$W = \frac{2\pi e^2 A_0^2}{\hbar m_c^2 c^2} \sum_{n} \sum_{k_{\|}} \left| u_A \bullet M_{CV}(k_{\|}) \right|^2 \left[f_c(E_{Ck_{\|}n}) - f_v(E_{Vk_{\|}n}) \right] \delta\left(E_{Vk_{\|}n} - E_{Ck_{\|}n} + \hbar\omega \right) \qquad (3.1.1\text{-}11)$$

where u_A is the unit vector along A_0 and corresponds to the polarization of the photon. Now, the allowed $k_{\|}$ vectors are distributed in the Brillouin zone with a surface density $A_{\|}/(2\pi)^2$ where $L_x L_y = A_{\|}$. The summation over $k_{\|}$-space is replaced by an integral extending over the first Brillouin zone. Hence, we have

$$W = \frac{2\pi e^2 A_0^2}{\hbar m_c^2 c^2} \sum_n \iint_{BZ} 2A_{\|} \frac{d^2k_{\|}}{(2\pi)^2} \left| u_A \bullet M_{CV}(k_{\|}) \right|^2 \left[f_c(E_{Ck_{\|}n}) - f_v(E_{Vk_{\|}n}) \right] \delta (E_{Vk_{\|}n} - E_{Ck_{\|}n} + \hbar\omega)$$

(3.1.1-12)

where we included a factor of 2 to account for electron spin.

The region in the energy band diagram under consideration is that of $k_{\|}$ very close to zero. We may therefore assume that the matrix element $|u_A \bullet M_{CV}(k_{\|})|^2 \approx |u_A \bullet M_{CV}(0)|^2$ is constant. Hence,

$$W = \frac{2\pi e^2 A_0^2 \left| u_A \bullet M_{CV}(0) \right|^2}{\hbar m_c^2 c^2} \frac{A_{\|}}{2\pi^2} \sum_n \iint_{BZ} d^2k_{\|} \left[f_c(E_{Ck_{\|}n}) - f_v(E_{Vk_{\|}n}) \right] \delta (E_{Vk_{\|}n} - E_{Ck_{\|}n} + \hbar\omega)$$

(3.1.1-13)

where $E_{Ck\|n}$ and $E_{Vk\|n}$ are given by (2.1.1-12a,b) in Chapter 2. All energies are measured from the bottom of the conduction band.

To perform the integration in (3.1.1-13), the double integral $d^2k_{\|}$ is changed to the single integral $2\pi k_{\|} dk_{\|}$, by assuming azimuthal symmetry. The expression (3.1.1-13) reduces to

$$W = \frac{2e^2A_0^2|\mathbf{u}_A \bullet M_{CV}(0)|^2 A_{||}}{\hbar m_c^2 c^2} \sum_n \int_0^\infty k_{||} dk_{||} \left[f_c(E_{Ck_{||}n}) - f_v(E_{Vk_{||}n}) \right] \delta(E_{Vk_{||}n} - E_{Ck_{||}n} + \hbar\omega)$$

(3.1.1-14)

For further simplification, the integration variable $k_{||}$ is changed to $\beta_{||}$, where

$$\beta_{||} = \frac{\hbar^2}{2m_r} k_{||}^2$$

and $m_r^{-1} = m_c^{-1} + m_v^{-1}$ is the reduced mass. Also, the energy terms change to

$$E_{Ck_{||}n} = \frac{m_r}{m_c}\beta_{||} + E_{cn}$$

$$E_{Vk_{||}n} = -\frac{m_r}{m_v}\beta_{||} - E_{vn} - E_g$$

Substituting the above into (3.1.1-14), we have

$$W = \frac{2e^2A_0^2|\mathbf{u}_A \bullet M_{CV}(0)|^2 A_{||}}{\hbar m_c^2 c^2} \sum_n \frac{m_r}{\hbar^2} \int_0^\infty d\beta_{||} \left[f_c\left(\frac{m_r}{m_c}\beta_{||} + E_{cn}\right) - f_v\left(-\frac{m_r}{m_v}\beta_{||} - E_{vn} - E_g\right) \right] \delta(-\beta_{||} - E_m - E_g + \hbar\omega)$$

(3.1.1-15)

where $E_{rn}=E_{cn}+E_{vn}$, and E_g is the 3D band gap energy. Now, the δ-function places a finite upper limit ($\hbar\omega-E_{rn}-E_g$) on the new integral. To integrate, we use the delta-function property

$$\int f(x)\,\delta(x-a)\,dx \;=\; f(a)$$

The total transition probability W per unit time given by (3.1.1-14) is now rewritten as

$$W = \frac{2e^2A_0^2\left|\mathbf{u}_A \bullet M_{CV}(0)\right|^2 A_{\|} m_r}{\hbar^3 m_c^2 c^2} \left[f_c\left\{(\hbar\omega - E_g)\frac{m_r}{m_c}\right\} - f_v\left\{(\hbar\omega - E_g)\frac{m_r}{m_c} - \hbar\omega\right\}\right] \sum_n H\left[\hbar\omega - E_m - E_g\right] \qquad (3.1.1\text{-}16)$$

where H is the Heaviside step function (defined in Chapter 2) and accounts for the integral over the δ-function.

3.1.2 Transition Probability in a 1D QW Laser

The procedure followed here is along the same lines as for the 2D QW laser. Choosing arbitrary initial and final states from the respective conduction and valence bands, electronic wavefunctions for the electron undergoing a transition are (from equation 2.2.1-13a,b)

$$\Psi_i = \Psi_{Ck_x mn}(x,y,z) = \frac{2}{\sqrt{L_y L_z N_u}} u_{Ck_x}(x) e^{ik_x x} CS\left(\frac{m\pi}{L_y} y\right) CS\left(\frac{n\pi}{L_z} z\right) \quad (3.1.2\text{-}1a)$$

$$\Psi_f = \Psi_{Vk'_x m'n'}(x,y,z) = \frac{2}{\sqrt{L_y L_z N_u}} u_{Vk'_x}(x) e^{ik'_x x} CS\left(\frac{m\pi}{L_y} y\right) CS\left(\frac{n'\pi}{L_z} z\right) \quad (3.1.2\text{-}1b)$$

Substituting these wavefunctions into (3.1-9), the matrix element $(M_{if})_{1D}$ for the 1D case is

$$(M_{if})_{1D} = \left\langle \Psi_{Vk'_x m'n'} \middle| e^{iq\bullet r} A_0 \bullet p \middle| \Psi_{Ck_x mn} \right\rangle$$

$$= \frac{4}{L_y L_z N_u} \iiint u^*_{Vk'_x}(x) e^{-ik'_x x} CS\left(\frac{m'\pi}{L_y} y\right) CS\left(\frac{n'\pi}{L_z} z\right) e^{iq\bullet r} A_0 \bullet p\, u_{Ck_x}(x) e^{ik_x x} CS\left(\frac{m\pi}{L_y} y\right) CS\left(\frac{n\pi}{L_z} z\right) d^3r \quad (3.1.2\text{-}2)$$

Following similar arguments to those in Section 3.1.1, the 3D position vector r(x,y,z) of a point (x,y,z) in the active region is rewritten thus:

$$r(x,y,z) = \hat{x}x + \hat{y}y + \hat{z}z = \hat{x}\{\rho_x + R_{xi}\} + \hat{y}y + \hat{z}z \quad (3.1.2\text{-}3)$$

where $\hat{x}R_{xi}$ determines the position of the 1D unit cell , and $\hat{x}\rho_x$ the displacement of the point relative to the 'address' $\hat{x}R_{xi}$ of the unit cell.

By substituting (3.1.2-3) into (3.1.2-2), the integral over the crystal is expressed as an integral over any unit cell summed over all unit cells (of total number N_u). Thus,

$$(M_{if})_{1D} = \frac{4}{L_y L_z N_u} \sum_{i=1}^{N_u} \iiint u^*_{Vk'_x}(\rho_x + R_{xi}) e^{-ik'_x(\rho_x + R_{xi})} CS\left(\frac{m'\pi}{L_y} y\right) CS\left(\frac{n'\pi}{L_z} z\right) e^{iq_x(\rho_x + R_{xi})} e^{i(q_y y + q_z z)} \mathbf{A}_0 \bullet \mathbf{p}$$
$$u_{Ck_x}(\rho_x + R_{xi}) e^{ik_x(\rho_x + R_{xi})} CS\left(\frac{m\pi}{L_y} y\right) CS\left(\frac{n\pi}{L_z} z\right) d\rho_x \, dy \, dz \qquad (3.1.2\text{-}4)$$

As with the 2D case, we may gather the exponential terms in R_{xi} outside the integral sign. The summation over *i* reduces to $N_u \, \delta(-k_x' + k_x + q_x)$, where the δ-function essentially ensures momentum conservation. Also, functions u_{Ck_x} and $u_{Vk'_x}$ being periodic with the same periodicity as the crystal, implies that

$$u_{Ck_x}(\rho_x + R_{xi}) = u_{Ck_x}(\rho_x)$$
$$u_{Vk'_x}(\rho_x + R_{xi}) = u_{Vk'_x}(\rho_x)$$

The above matrix element expression in (3.1.2-4) thus simplifies to

$$(M_{if})_{1D} = \frac{4}{L_y L_z}\,\delta(-k'_x + k_x + q_x)$$

$$\iiint_{\text{any unit cell}} u^{*}_{Vk'_x}(\rho_x)\, e^{-ik'_x\rho_x}\, CS\left(\frac{m'\pi}{L_y}y\right) CS\left(\frac{n'\pi}{L_z}z\right)\, e^{iq_x\rho_x}\, e^{i(q_y y + q_z z)}$$

$$A_0 \bullet \mathbf{p}\, u_{Ck_x}(\rho_x)\, e^{ik_x\rho_x}\, CS\left(\frac{m\pi}{L_y}y\right) CS\left(\frac{n\pi}{L_z}z\right) d\rho_x\, dy\, dz \qquad (3.1.2\text{-}5)$$

As in Section 3.1.1, we may write

$$\mathbf{p}\, u_{Ck_x}(\rho_x)\, e^{ik_x\rho_x}\, CS\left(\frac{m\pi}{L_y}y\right) CS\left(\frac{n\pi}{L_z}z\right)$$

$$= e^{ik_x\rho_x}\,(\hbar k_x + \mathbf{p})\, u_{Ck_x}(\rho_x)\, CS\left(\frac{m\pi}{L_y}y\right) CS\left(\frac{n\pi}{L_z}z\right)$$

Substituting the above into (3.1.2-5) and using the momentum δ-function, we allow $e^{i(-k'_x + k_x - q_x)} = 1$. At this stage, for reasons outlined in Section 3.1.1, we further assume that photon momentum **q** is much smaller in magnitude than the wave vectors **k'**, **k**. Only "vertical" transitions are induced in the energy band diagram by the radiation field. Also, including the orthonormality of Bloch functions, (3.1.2-5) reduces to

$$(M_{if})_{1D} = \frac{4}{L_y L_z}\,\delta(k_x - k'_x) \iiint_{\text{any unit cell}} u^{*}_{Vk'_x}(\rho_x)\, CS\left(\frac{m'\pi}{L_y}y\right) CS\left(\frac{n'\pi}{L_z}z\right)$$

$$A_0 \bullet \mathbf{p}\, u_{Ck_x}(\rho_x) CS\left(\frac{m\pi}{L_y}y\right) CS\left(\frac{n\pi}{L_z}z\right) d\rho_x\, dy\, dz \qquad (3.1.2\text{-}6)$$

As before, we expand the momentum operator $\mathbf{p} = \hat{x}p_x + \hat{y}p_y + \hat{z}p_z$ to obtain

$$\mathbf{p}\, u_{Ck_x}(\rho_x)\, CS\left(\frac{m\pi}{L_y}y\right) CS\left(\frac{n\pi}{L_z}z\right) = CS\left(\frac{m\pi}{L_y}y\right) CS\left(\frac{n\pi}{L_z}z\right) \hat{x}\, p_x\, u_{Ck_x}(\rho_x)$$
$$+ \; u_{Ck_x}(\rho_x) \left\{ \pm i\hbar \left[\frac{m\pi}{L_y} SC\left(\frac{m\pi}{L_y}y\right) CS\left(\frac{n\pi}{L_z}z\right) + \frac{n\pi}{L_z} SC\left(\frac{n\pi}{L_z}z\right) CS\left(\frac{m\pi}{L_y}y\right) \right] \right\}$$

Substituting the above into (3.1.2-6), the terms within the curly brackets go to zero under the y- and z-integrations, respectively. Thus, (3.1.2-6) is

$$(M_{if})_{1D} = \delta_{mm'}\, \delta_{nn'}\, \delta(k_x - k'_x)\, A_0 \bullet \hat{x} M_{CV}(k_x) \qquad (3.1.2\text{-}7)$$

where $M_{CV}(k_x)$ is the matrix element given by

$$M_{CV}(k_x) = \int_{\substack{\text{any 1D} \\ \text{unit cell}}} u^*_{Vk_x}(\rho_x)\, p_x\, u_{Ck_x}(\rho_x)\, d\rho_x \qquad (3.1.2\text{-}8)$$

and the Kronecker delta functions $\delta_{mm'}$ and $\delta_{nn'}$ appear due to the orthonormality of the CS functions.

At this stage, we recall the expression for the total transition probability given by (3.1-12). The initial state summation implies summations over k_x', m' and n', while the final state summation over k_x, m and n. Substituting (3.1.2-7) into (3.1-12), we sum over k_x', m' and n' using the respective δ-

functions. The total transition probability W per unit time for the net emission of photons of frequency ω is now simply

$$W = \frac{2\pi e^2 A_0^2}{\hbar m_c^2 c^2} \sum_{m,n} \sum_{k_x} \left| \mathbf{u}_A \cdot \hat{\mathbf{x}} M_{CV}(k_x) \right|^2 \left[f_c(E_{Ck_x mn}) - f_v(E_{Vk_x mn}) \right] \delta (E_{Vk_x mn} - E_{Ck_x mn} + \hbar\omega) \tag{3.1.2-9}$$

where $\mathbf{u}_A$ corresponds to the photon polarization. Now, the allowed k_x vectors are distributed in the Brillouin zone with a linear density $L_x/2\pi$. The summation over k_x-space is replaced by an integral extending over the first Brillouin zone. We include a factor of 2 to account for electron spin, and assume that $|\mathbf{u}_A \cdot \hat{\mathbf{x}} M_{CV}(k_x)|^2 \approx |\mathbf{u}_A \cdot \hat{\mathbf{x}} M_{CV}(0)|^2$ is constant. Hence,

$$W = \frac{2\pi e^2 A_0^2 \left| \mathbf{u}_A \cdot \hat{\mathbf{x}} M_{CV}(0) \right|^2}{\hbar m_c^2 c^2} \sum_{m,n} 2 \int_0^{\infty} 2L_x \frac{dk_x}{2\pi} \left[f_c(E_{Ck_x mn}) - f_v(E_{Vk_x mn}) \right] \delta (E_{Vk_x mn} - E_{Ck_x mn} + \hbar\omega) \tag{3.1.2-10}$$

where the energies $E_{Ck_x mn}$ and $E_{Vk_x mn}$ are given by (2.2.1-14a, b) in Chapter 2. All energies are measured as before.

To perform the integration in (3.1.2-10), the integration variable k_x is changed to β_x, where

$$k_x = \left(\frac{2m_r}{\hbar^2}\right)^{\frac{1}{2}} \beta_x^{\frac{1}{2}}$$

and $m_r^{-1} = m_c^{-1}+m_v^{-1}$ is the reduced mass. The energy terms are rewritten as

$$E_{Ck_xmn} = \frac{m_r}{m_c}\beta_x + E_{cmn}$$
$$E_{Vk_xmn} = -\frac{m_r}{m_v}\beta_x - E_{vmn} - E_g$$

Substituting the above into (3.1.2-10), we have

$$W = \frac{4e^2A_0^2\left|u_A \cdot \hat{x} M_{CV}(0)\right|^2 L_x}{\hbar m_c^2 c^2} \sum_n \left(\frac{m_r}{2\hbar^2}\right)^{\frac{1}{2}}$$
$$\int_0^\infty d\beta_x\, \beta_x^{-\frac{1}{2}} \left[f_c\left\{\beta_x \frac{m_r}{m_c} + E_{cmn}\right\} - f_v\left\{-\beta_x \frac{m_r}{m_v} - E_{vmn} - E_g\right\}\right]$$
$$\delta(-\beta_x + \hbar\omega - E_{rmn} - E_g) \qquad (3.1.2\text{-}11)$$

where $E_{rmn}=E_{cmn}+E_{vmn}$, and E_g is the 3D bulk band gap energy. Once again, the δ-function places a finite upper limit ($\hbar\omega$-E_{rmn}-E_g) on the new integral. Using the delta-function property given by (3.1.2-11), the total transition probability W per unit time reduces to

$$W = \frac{2e^2A_0^2\left|u_A \bullet M_{CV}(0)\right|^2 L_x (2m_r)^{\frac{1}{2}}}{\hbar^2 m_c^2 c^2} \left[f_c\left\{(\hbar\omega - E_g)\frac{m_r}{m_c}\right\} - f_v\left\{(\hbar\omega - E_g)\frac{m_r}{m_c} - \hbar\omega\right\}\right] \sum_{m,n} (\hbar\omega - E_g - E_{rmn})^{-\frac{1}{2}} H\left[\hbar\omega - E_g - E_{rmn}\right] \quad (3.1.2\text{-}12)$$

where the Heaviside function **H** accounts for the integral over the δ-function.

3.2 Gain in Quantum Well Lasers

Optical gain of the QW laser is essentially the net photon emission (*i.e.* difference of photon absorption and photon emission), neglecting any coupling and cavity losses. It is determined through a relationship between optical constants, which describe the optical properties of matter, and the transition probability W(ω). The average energy density u of an EM radiation field described by the vector potential **A** of (3.1-3) in a medium is related to the optical constants through the following[28]:

$$u(\omega) = \frac{\varepsilon_0 n_r^2 A_0^2 \omega^2}{2c^2} \quad (3.2\text{-}1)$$

where n_r is the refractive index of the medium and c the velocity of light in vacuum. The gain coefficient is defined as the net EM energy emitted in unit

time per unit volume $\hbar\omega W(\omega)/V$ divided by the energy flux $u(c/n_r)$ in the medium. We therefore write

$$\gamma(\omega) \equiv \alpha(\omega) = \frac{\hbar\omega W(\omega)}{u(c/n_r)V} \tag{3.2-2}$$

Substituting (3.2-1) into (3.2-2),

$$\gamma(\omega) = \frac{2c\hbar W(\omega)}{\varepsilon_0 n_r A_0^2 \omega V} \tag{3.2-3}$$

We now derive explicit expressions for the gain coefficient for 2D and 1D QW lasers.

3.2.1 Gain Coefficient for the 2D QW Laser

The gain coefficient for the 2D QW laser is obtained by substituting the transition probability for the 2D case $W_{2D}(\omega)$ from (3.1.1-16) into (3.2-3). We thus have

$$\gamma_{2D}(\omega) = \frac{4e^2\left|\hat{u}_A \bullet M_{CV}(0)\right|^2 m_r}{\omega\varepsilon_0 n_r c m_c^2 \hbar^2 L_z} \left[f_c\left\{(\hbar\omega - E_g)\frac{m_r}{m_c}\right\} - f_v\left\{(\hbar\omega - E_g)\frac{m_r}{m_c} - \hbar\omega\right\}\right] \sum_n H\left[\hbar\omega - E_g - E_m\right] \tag{3.2.1-1}$$

To simplify the above expression, we write the momentum matrix element $M_{CV}(0)$ in terms of the electric dipole moment matrix element μ as follows,

$$\left|\hat{u}_A \bullet M_{CV}(0)\right| = -\frac{\omega m_c}{i e}\mu \qquad (3.2.1\text{-}2)$$

where μ has the same polarization as the photon. Substituting the above into (3.2.1-1), we have

$$\gamma_{2D}(\omega) = \frac{8\pi\mu^2 m_r}{\lambda \varepsilon_0 n_r \hbar^2 L_z}\left[f_c\left\{(\hbar\omega - E_g)\frac{m_r}{m_c}\right\} - f_v\left\{(\hbar\omega - E_g)\frac{m_r}{m_c} - \hbar\omega\right\}\right] \sum_n H\left[\hbar\omega - E_g - E_m\right] \qquad (3.2.1\text{-}3)$$

in which we also replaced ω outside the summation sign by its equivalent in photon wavelength λ ($\omega = 2\pi c/\lambda$). The above expression agrees with the result derived from the imaginary part of the complex susceptibility in Chapter 12 of reference 13.

Plots on the following pages show the theoretical variation of the 2D gain coefficient with photon frequency, as other parameters (well width, temperature, concentration) are changed. The Fortran program listed in Appendix A was written to calculate gain values. This program (and all others following) were run on a "Macintosh Classic" computer. These graphs

(and all other graphs to follow) were generated using the "Cricket Graph 1.3" graphics package on the same computer.

Figure 3-1 shows a graph of the 2D optical gain coefficient per unit volume plotted versus net transition energy (difference of photon energy and band gap energy) at fixed temperature and well width for various carrier concentrations N_0. It depicts the expected result that gain increases with carrier concentration.

In Figure 3-2, we have plotted the maximum gain coefficient values versus carrier concentration. Since the charge carrier concentration is directly related to the threshold current density J through the following relationship[13],

$$J = \frac{eN_0L_z}{\tau}$$

this variation in gain is directly proportional to the threshold current density. Here, 'e' is the electronic charge, and τ the density-independent carrier lifetime. As compared to an ordinary DH-junction laser[13] (J ~1000A/cm^3), the threshold current density is considerably lower[13] (J ~100A/cm^3) in the 2D QW laser case.

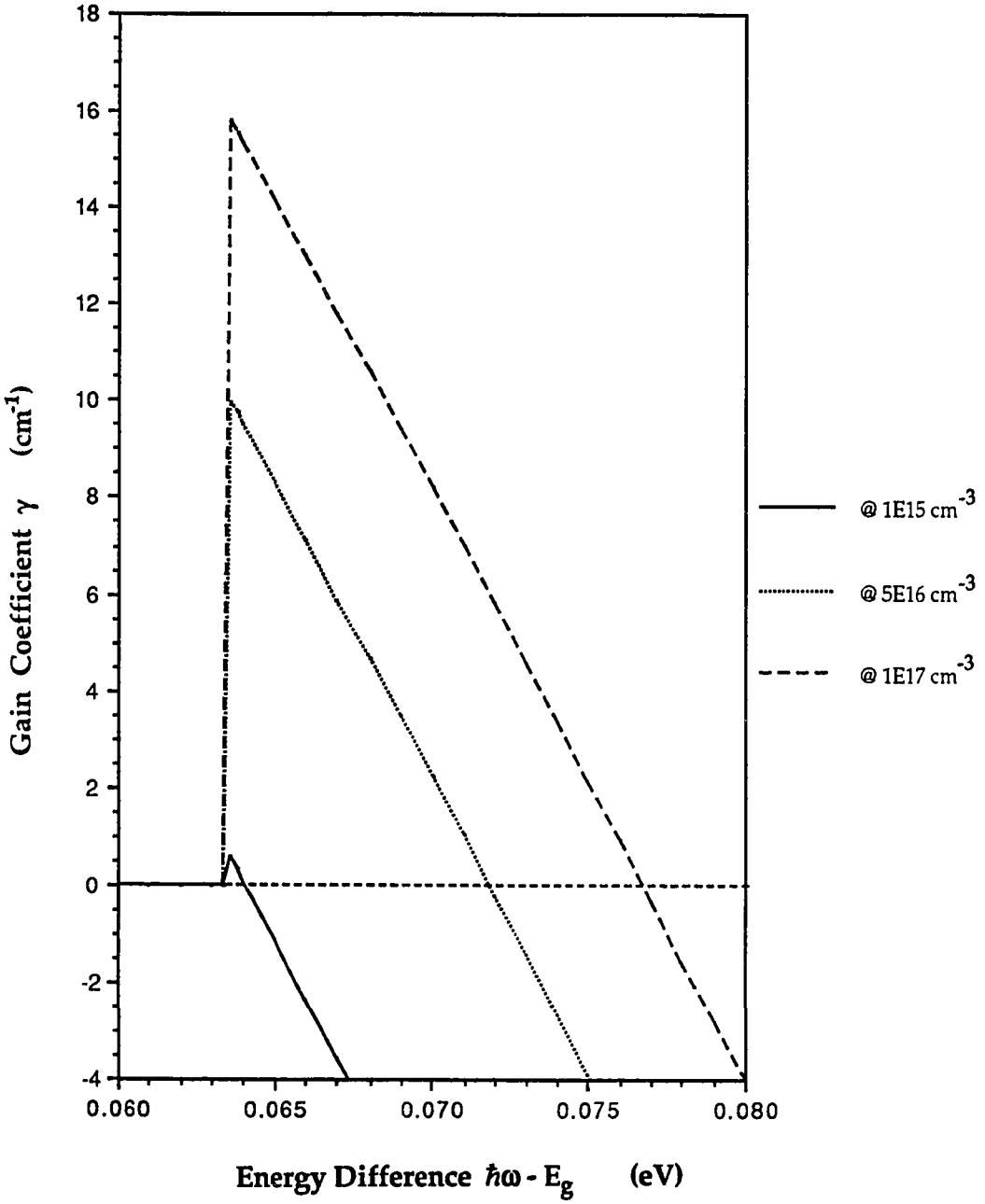

Figure 3-1: Optical gain coefficient per unit volume of a 2D QW structure plotted versus net transition energy at fixed temperature (T = 300 K) and well width (L_z = 100 Å) for various carrier concentrations N_0. Here, the k-selection rule is obeyed.

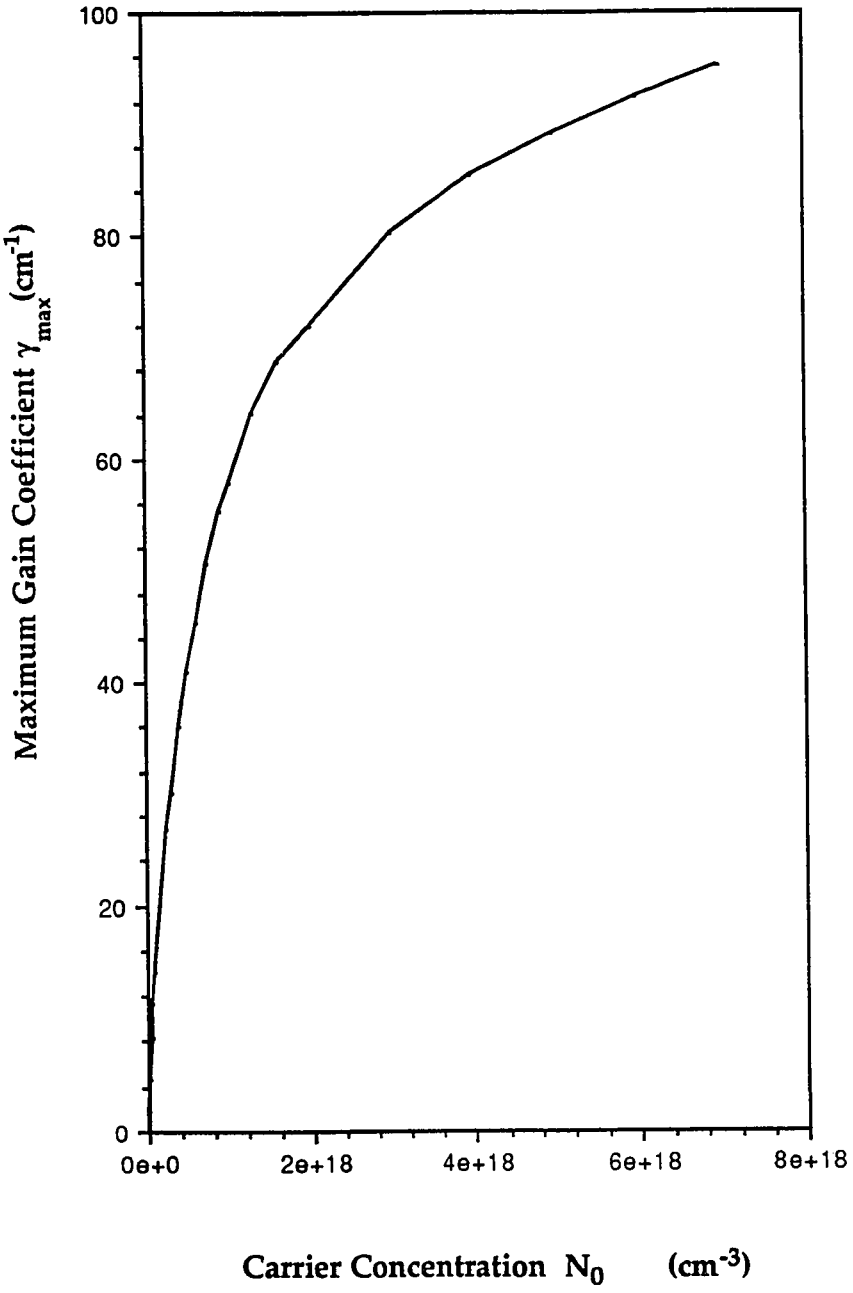

Figure 3-2: Maximum optical gain coefficient per unit volume for a 2D QW structure plotted versus carrier concentration N_0 at fixed temperature (T = 300 K) and well width (L_z = 100 Å). The k-selection rule is obeyed here.

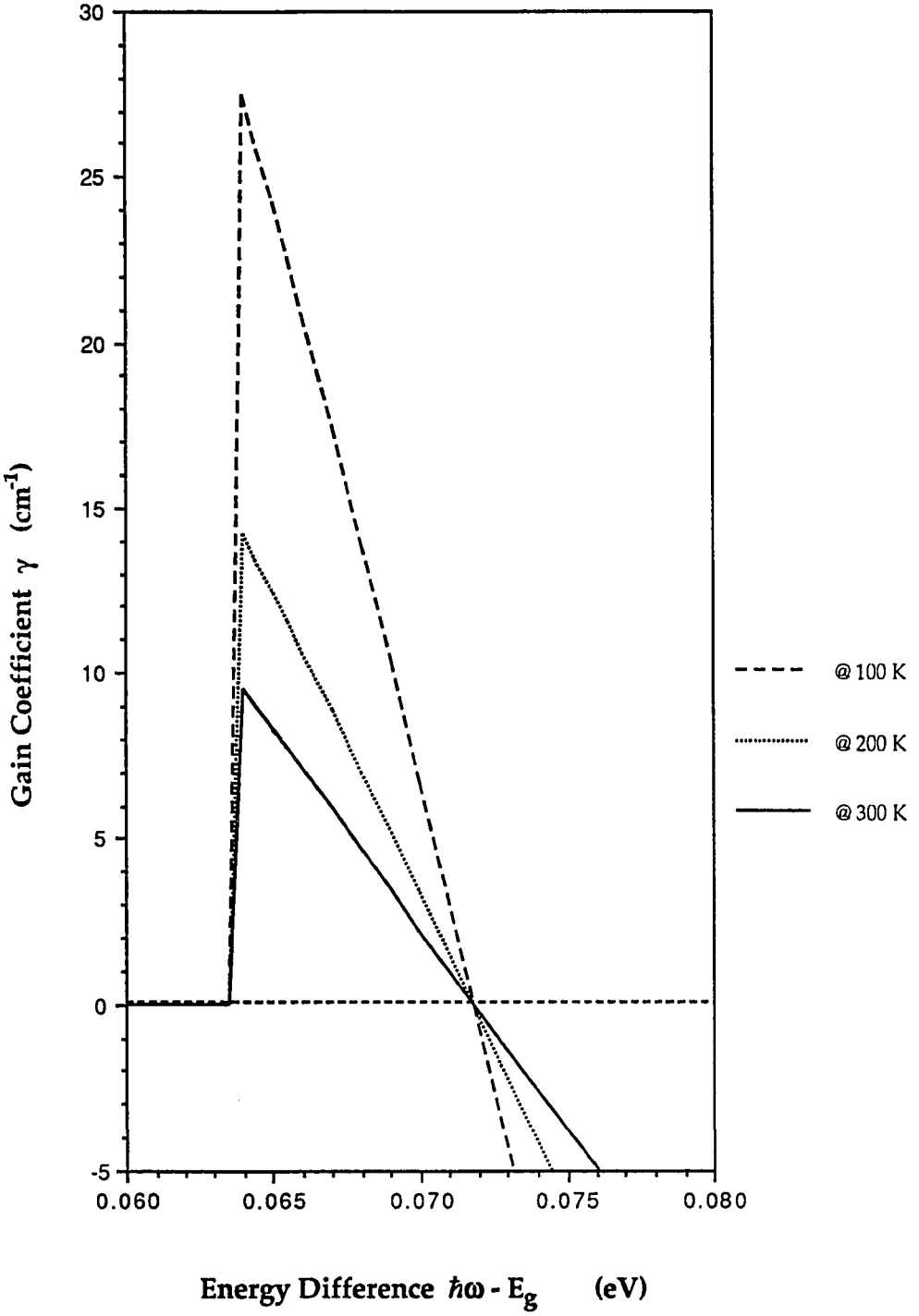

Figure 3-3: Optical gain coefficient per unit volume of a 2D QW structure plotted versus net transition energy at fixed carrier concentration (N_0 = 5E16 cm^{-3}) and well width (L_z = 100 Å) for various temperatures T. The k-selection rule is obeyed here.

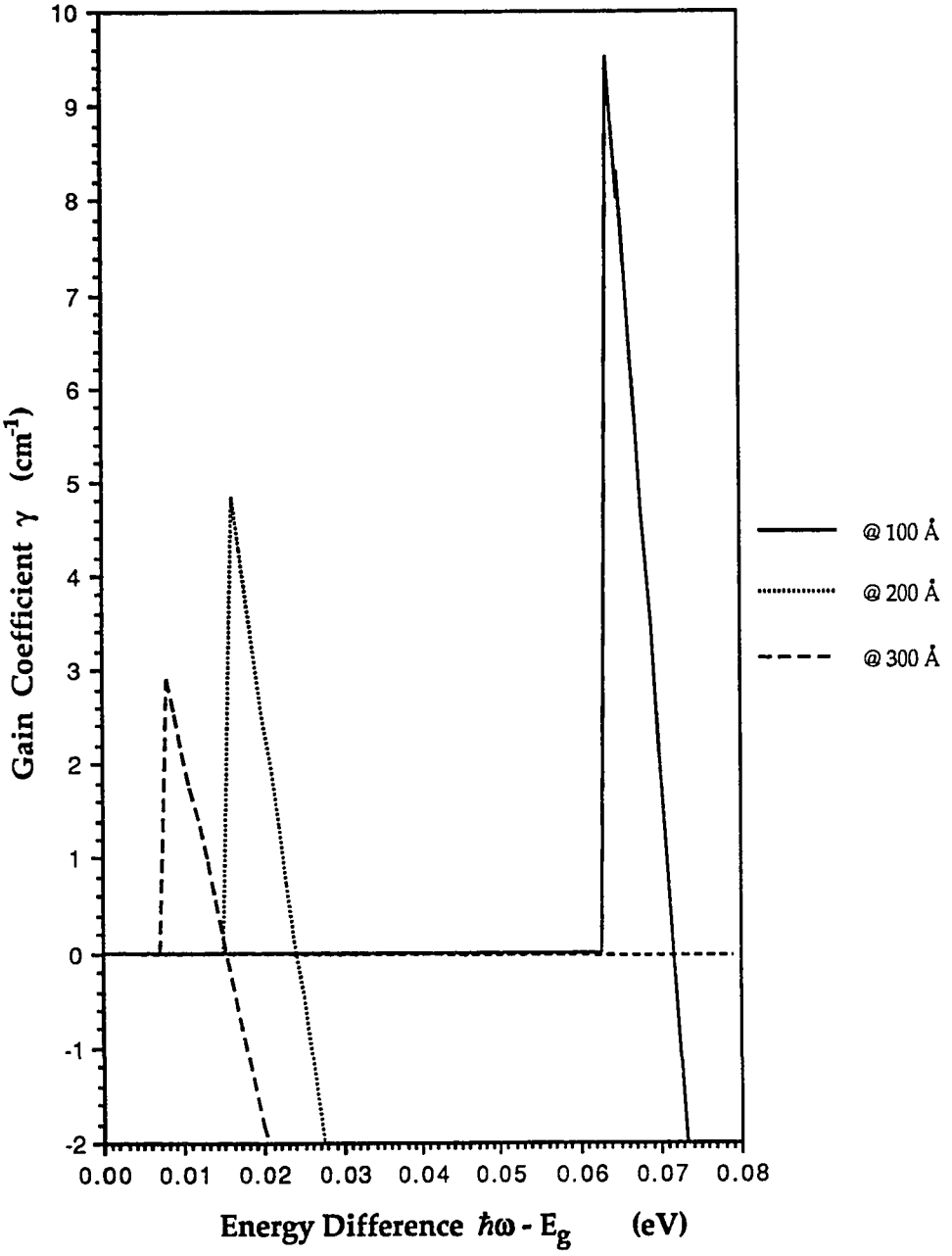

Figure 3-4: Optical gain coefficient per unit volume of a 2D QW structure plotted versus net transition energy at fixed carrier concentration (N_0 = 5E16 cm^{-3}) and temperature (T= 300 K) for various well widths L_z. Here, the k-selection rule is obeyed.

The latter figures show that optical gain is greater at lower temperatures {Figure 3-3}, and at smaller well widths {Figure 3-4}. Both results are intuitive. At lower temperatures, more charge carriers exist in the lowest conduction and valence bands. Since transitions between these bands contribute the most towards optical gain, the gain is larger. Also, at lower temperatures, losses due to heat and tunneling are smaller. The larger gain at smaller well width is an obvious result of the gain coefficient expression, where $\gamma(\omega)$ varies inversely as L_z.

3.2.2 Gain Coefficient for the 1D QW laser

As in Section 3.1.1, substituting the transition probability $W_{1D}(\omega)$ from (3.1.2-12) into expression (3.2-3), the 1D gain coefficient is written as

$$\gamma_{1D}(\omega) = \frac{8\pi(2m_r)^{1/2}\mu^2}{\lambda\varepsilon_0 n_r \hbar L_y L_z}\left[f_c\left\{\left(\hbar\omega - E_g\right)\frac{m_r}{m_c}\right\} - f_v\left\{\left(\hbar\omega - E_g\right)\frac{m_r}{m_c} - \hbar\omega\right\}\right] \sum_{m,\,n}\left(\hbar\omega - E_g - E_{rmn}\right)^{-\frac{1}{2}} H\left[\hbar\omega - E_g - E_{rmn}\right] \tag{3.2.2-1}$$

where we have used (3.2.1-2), $V = L_xL_yL_z$, and $\omega = 2\pi c/\lambda$.

Plots on the following pages show the theoretical variation of the 1D gain coefficient with photon frequency, as different parameters are changed. A Fortran program (Appendix B) was written to make calculations.

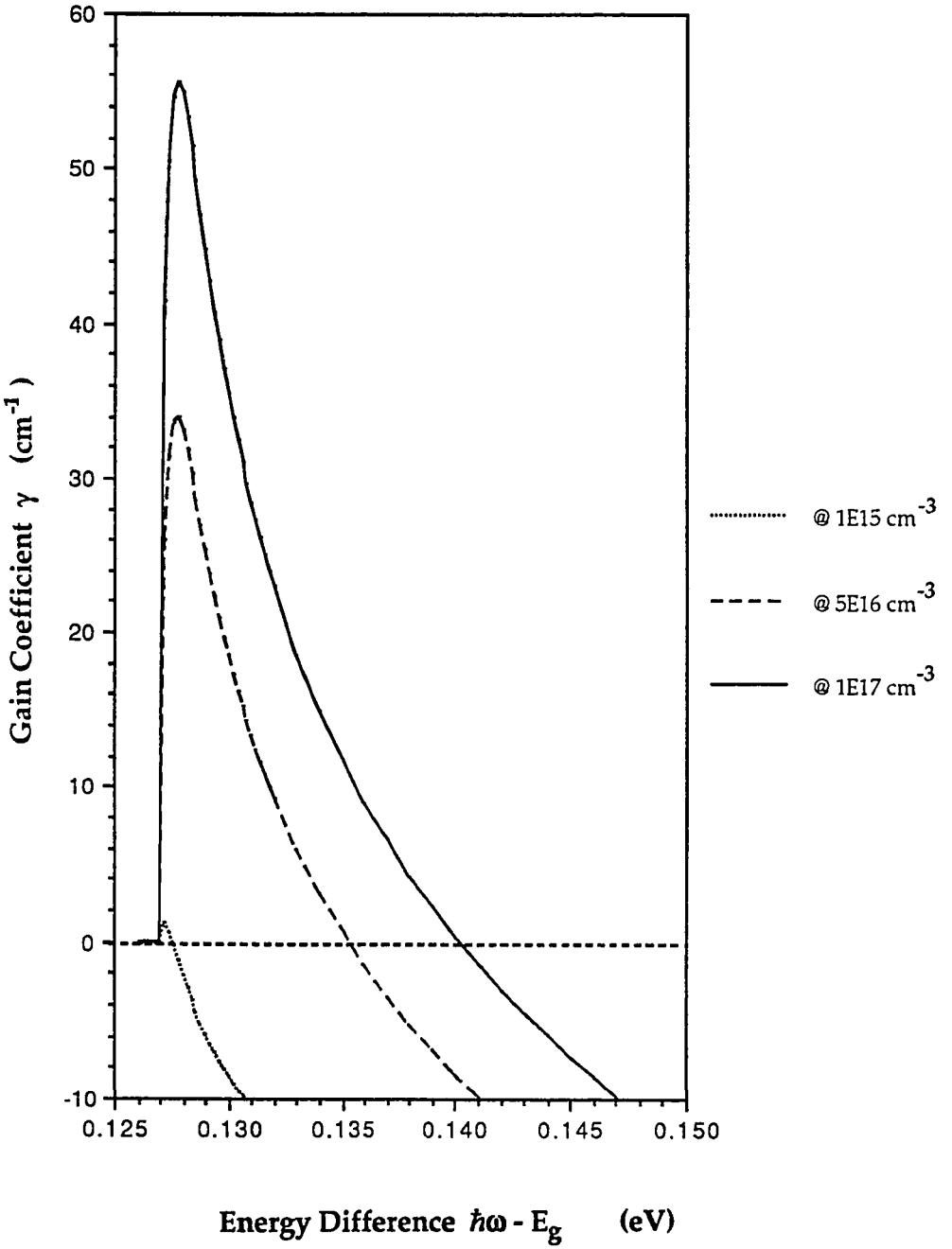

Figure 3-5: Optical gain coefficient per unit volume of a 1D QW structure plotted versus net transition energy at fixed temperature (T = 300 K) and well widths ($L_y = L_z$ =100 Å) for various carrier concentrations N_0. Here, the k-selection rule is obeyed.

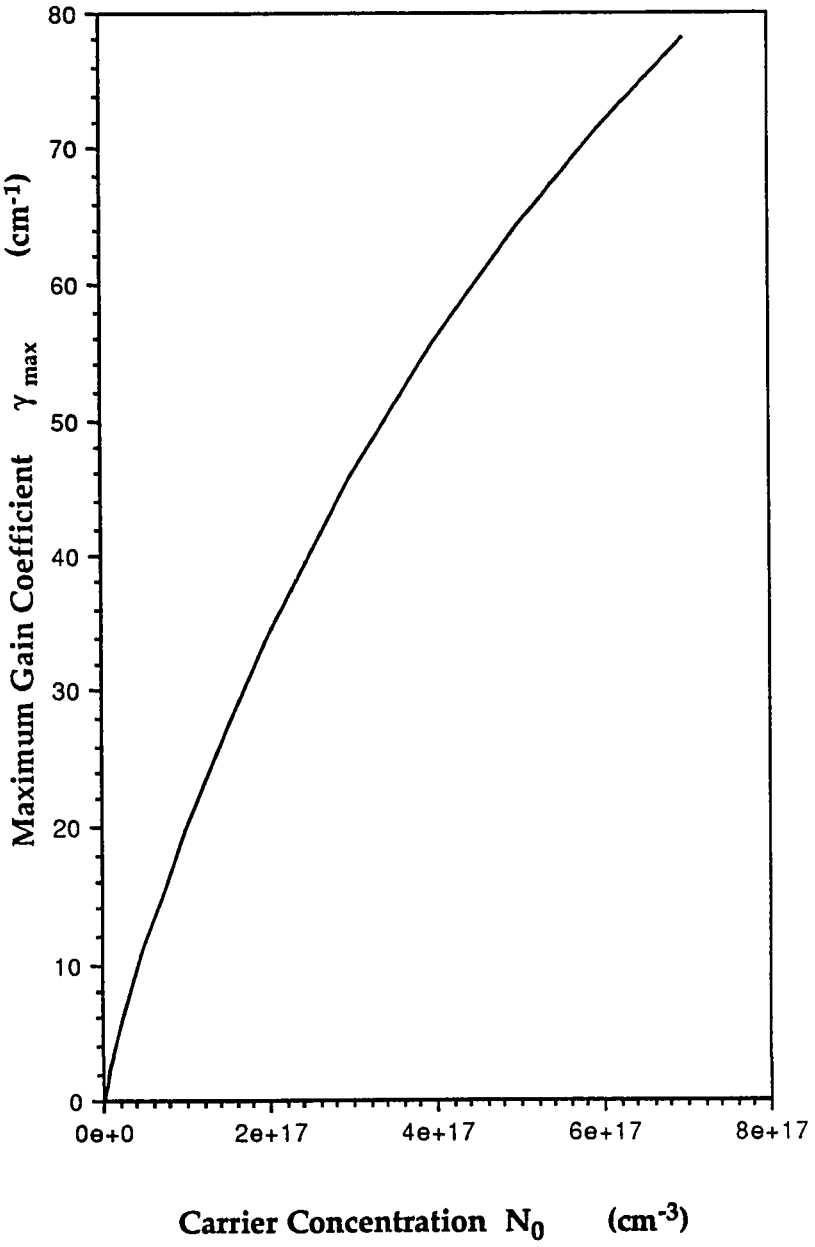

Figure 3-6: Maximum optical gain coefficient per unit volume for a 1D QW structure plotted versus carrier concentration N_0 at fixed temperature (T = 300 K) and well widths ($L_y = L_z = 100$ Å). The k-selection rule is obeyed here.

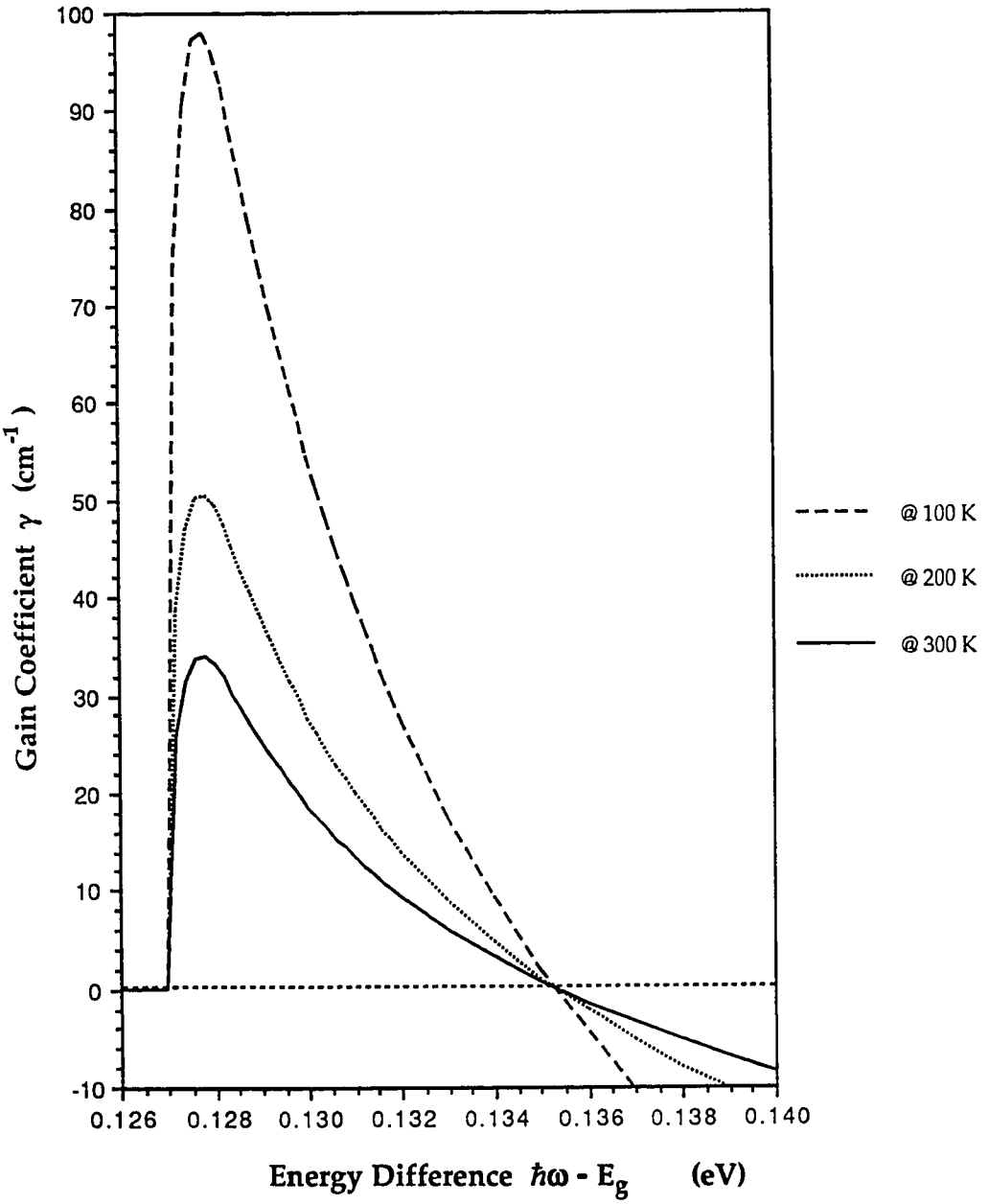

Figure 3-7: Optical gain coefficient per unit volume of a 1D QW structure plotted versus net transition energy at fixed carrier concentration (N_0 = 5E16 cm^{-3}) and well width ($L_y = L_z$ = 100 Å) for various temperatures T. The k-selection rule is obeyed here.

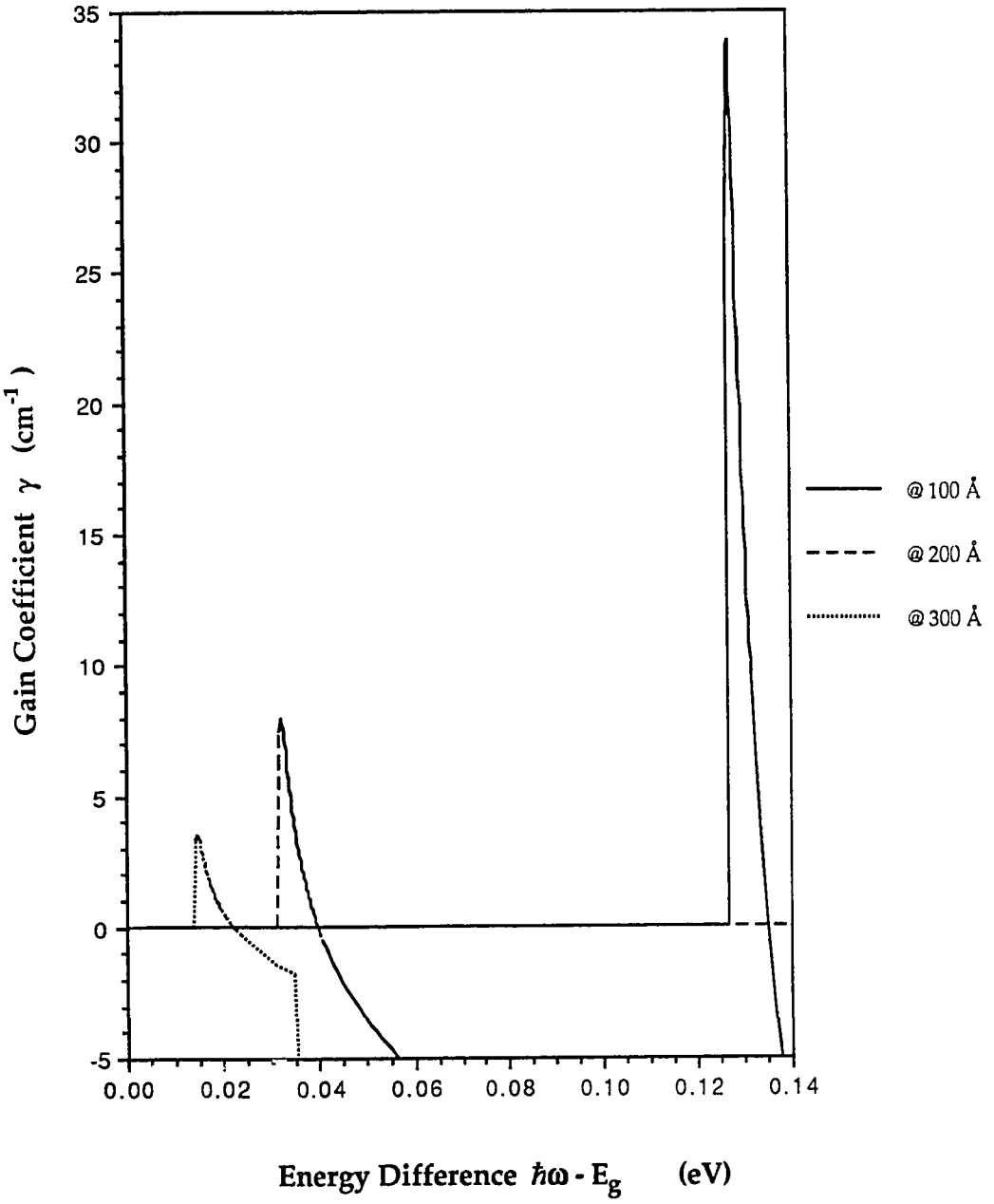

Figure 3-8: Optical gain coefficient per unit volume of a 1D QW structure plotted versus net transition energy at fixed carrier concentration (N_0 = 5E16 cm^{-3}) and temperature (T= 300 K) for various well widths $L_y = L_z$. Here, the k-selection rule is obeyed.

Here, we prevent the gain calculations from approaching singularities (division by zero at $\hbar\omega \approx E_g + E_{rmn}$) by adding a small damping factor. Physically, this damping factor is related to the finite uncertainty in determining the energy band levels.

As in the 2D situation, the volumetric 1D optical gain is greater at larger carrier concentrations, smaller temperatures and smaller well widths. Physical reasons for these observations are the same as outlined in the 2D case.

3.3 Relationship between 3D, 2D, and 1D Optical Gains

A simple comparison of the 3D, 2D, and 1D gain coefficient values obtained explicitly shows that the optical gain increases with decrease in dimension. As mentioned in Chapter 2, bulk and QW lasers are usually operated close to threshold. However, the threshold frequencies in the three cases are not the same, since the effective band gap energies differ due to quantization. The 3D active region has the smallest band gap energy (E_g), followed by the 2D QW active region (E_g+E_{r1}), and the 1D region has the largest band gap energy (E_g+E_{r11}). Energies E_{r1} and E_{r11} have been defined in Chapter 2. We therefore compare all gain coefficients at their respective threshold frequencies.

Consider a ratio of the 1D gain coefficient to the 2D gain coefficient near their respective threshold frequencies:

$$\frac{\gamma_{1D}\left(\omega\to\frac{1}{\hbar}\left[E_g+E_{r11}\right]\right)}{\gamma_{2D}\left(\omega\to\frac{1}{\hbar}\left[E_g+E_{r1}\right]\right)}=\frac{\left|f_c\left\{(\hbar\omega-E_g)\frac{m_r}{m_c}\right\}-f_v\left\{(\hbar\omega-E_g)\frac{m_r}{m_c}-\hbar\omega\right\}\right|}{\left[f_c\left\{(\hbar\omega-E_g)\frac{m_r}{m_c}\right\}-f_v\left\{(\hbar\omega-E_g)\frac{m_r}{m_c}-\hbar\omega\right\}\right]}$$

$$\times\ \frac{2}{\pi}\sqrt{\frac{\pi^2\hbar^2}{2m_rL_y^2}}\ \frac{\sum_{m,n}\left(\hbar\omega-E_g-E_{rmn}\right)^{-\frac{1}{2}}\ \mathbf{H}\left[\hbar\omega-E_g-E_{rmn}\right]}{\sum_{n}\ \mathbf{H}\left[\hbar\omega-E_g-E_{rn}\right]}$$

The Fermi inversion factors are identical and cancel each other. For $L_y=L_z$, if the 1D Heaviside function condition is satisfied, then the 2D Heaviside function condition is also necessarily satisfied. Thus, for the condition $\hbar\omega > E_g + E_{r11}$, we have

$$\frac{\gamma_{1D}\left(\omega\to\frac{1}{\hbar}\left[E_g+E_{r11}\right]\right)}{\gamma_{2D}\left(\omega\to\frac{1}{\hbar}\left[E_g+E_{r1}\right]\right)}=\frac{2}{\pi}\sqrt{\frac{\pi^2\hbar^2}{2m_rL_y^2}}\ \sum_{m,n}\left(\hbar\omega-E_g-E_{rmn}\right)^{-\frac{1}{2}}$$

$$\equiv\frac{\rho_{1D}\left(\omega\to\frac{1}{\hbar}\left[E_g+E_{r11}\right]\right)}{\rho_{2D}\left(\omega\to\frac{1}{\hbar}\left[E_g+E_{r1}\right]\right)}$$

i.e. the ratio of the above gain coefficients is exactly equal to the ratio of the respective densities of states near threshold. We notice that at threshold, *i.e.* $\hbar\omega \to E_g + E_{r11}$ and $m=n\to1$, the above ratio tends to infinity for small L_y. In other words, the optical gain increases infinitely in theory by reducing the QW laser dimension from 2D to 1D.

A ratio of the 2D gain coefficient with the 3D gain coefficient exhibits a similar result for $\hbar\omega \geq E_g + E_{r1}$, shown as follows:

$$\frac{\gamma_{2D}\left(\omega \to \frac{1}{\hbar}\left[E_g + E_{r1}\right]\right)}{\gamma_{3D}\left(\omega \to \frac{1}{\hbar}\left[E_g\right]\right)} = \sqrt{\frac{\pi^2\hbar^2}{2m_r L_z^2}}\left(\hbar\omega - E_g\right)^{-\frac{1}{2}} \cong \frac{\rho_{2D}\left(\omega \to \frac{1}{\hbar}\left[E_g + E_{r1}\right]\right)}{\rho_{3D}\left(\omega \to \frac{1}{\hbar}\left[E_g\right]\right)}$$

Again, at threshold, *i.e.* $\hbar\omega \to E_g + E_{r1}$ and $n \to 1$, the above ratio is infinitely large for small L_z (in theory) due to the density of states being quantized in 2D.

Under a strict k-selection rule, the optical gain of a 1D QW laser is theoretically shown to be larger than that of a 2D QW laser, which, in turn, is larger than the bulk gain. In the next chapter, we use a more realistic approach to calculate optical gain, where the system momentum is not conserved.

CHAPTER 4: OPTICAL GAIN IN QW LASERS WITH NO k-SELECTION RULE

In the previous chapter, we calculated the optical gain for QW structures by considering transitions between Bloch states corresponding to the valence and conduction bands. Assuming the photon wave vector **q** to be very small with respect to the Brillouin zone, we considered almost vertical transitions. This essentially describes the situation in which momentum is conserved during band-to-band transitions (*i.e.*, the **k**-selection rule holds).

However, evidence shows that the theoretical optical gain determined by strictly using the k-selection rule does not agree with all experiments. An earlier proposal by Lasher *et al.*[33] argued that this discrepancy may be due to the presence of random impurities in the material of QW structures. The consequential elastic scattering of charge carriers causes a breakdown of the momentum conservation rule. Other reasons for the k-selection rule to breakdown can be variations in well width and Al molar fraction through the active region, and a finite relaxation time. In real systems, one may expect partial momentum conservation, which allows a range of wavevectors to be involved in a transition. Using the two extreme cases of (i) strict k-selection, and (ii) no k-selection, certain research groups[15,33,34] have obtained a good theoretical fit for 2D QW gain spectra with reported experiments.

Essentially, the no k-selection rule implies that an electron can make non-vertical transitions in the energy band diagram, as long as the energy conservation rule is obeyed (see Figure 4-1 below).

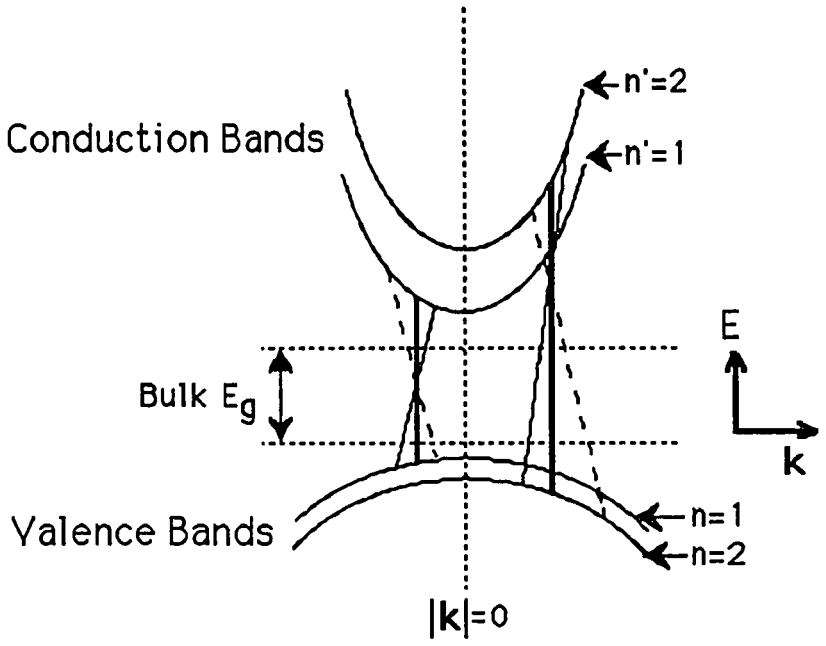

Figure 4-1: Energy diagram of a GaAs/$Ga_{1-x}Al_xAs$ QW laser showing vertical and non-vertical transitions due to the breakdown of the k-selection rule.

We now derive expressions for gain coefficients in 2D and 1D QW systems without assuming the k-selection rule.

4.1 The Two-dimensional Laser System

Having assumed that impurities are present in the lasing medium, we cannot use the wavefunctions given by (2.2.1-13a,b) to describe electron and

hole motions. This is because the crystal periodicity is broken by the impurities, and a purely Bloch state cannot exist. Thus, the wavefunctions are chosen as follows;

$$\Psi_{Ck_{\|}n}(\mathbf{r}_{\|}, z) = \sqrt{\frac{2}{L_z}}\,\phi_{Ck_{\|}}(\mathbf{r}_{\|})\,CS\left(\frac{n\pi}{L_z}z\right) \tag{4.1-1a}$$

$$\Psi_{Vk_{\|}'n}(\mathbf{r}_{\|}, z) = \sqrt{\frac{2}{L_z}}\,\phi_{Vk_{\|}'}(\mathbf{r}_{\|})\,CS\left(\frac{n\pi}{L_z}z\right) \tag{4.1-1b}$$

where

$$\phi_{Ck_{\|}}(\mathbf{r}_{\|}) = \sum_{k_{\|}} a_{k_{\|}} u_{Ck_{\|}}(\mathbf{r}_{\|})\, e^{i\mathbf{k}_{\|}\bullet\mathbf{r}_{\|}} \tag{4.1-2a}$$

$$\phi_{Vk_{\|}'}(\mathbf{r}_{\|}) = \sum_{k_{\|}'} a_{k_{\|}'} u_{Vk_{\|}'}(\mathbf{r}_{\|})\, e^{i\mathbf{k}_{\|}'\bullet\mathbf{r}_{\|}} \tag{4.1-2b}$$

are normalized functions consisting of Bloch-type wavefunctions of the impurity molecules superimposed on the pure material Bloch state.

We start with expression (3.1.1-2) from Chapter 3 for the matrix element before momentum conservation has been used. We have

$$\begin{aligned}(M_{if})_{2D} &= \left\langle \Psi_{Vk_{\|}'n'} \middle| e^{i\mathbf{q}\bullet\mathbf{r}}\,\mathbf{A}_0\bullet\mathbf{p} \middle| \Psi_{Ck_{\|}n} \right\rangle \\ &= \frac{2}{L_z}\iiint \phi^{*}_{Vk_{\|}'}(\mathbf{r}_{\|})\,CS\left(\frac{n'\pi}{L_z}z\right) e^{i\mathbf{q}\bullet\mathbf{r}}\,\mathbf{A}_0\bullet\mathbf{p}\,\phi_{Ck_{\|}}(\mathbf{r}_{\|})\,CS\left(\frac{n\pi}{L_z}z\right) d^3r\end{aligned} \tag{4.1-3}$$

Directly making the assumption that the photon momentum **q** is much smaller in magnitude than the wave vectors **k** and **k'**, we approximate $e^{i\mathbf{q}\cdot\mathbf{r}}$ to 1. Then, separating the z-integration from the $k_{||}$-integration, we assume that transitions occur between bands of identical quantum number only, and obtain the Kronecker δ-function $\delta_{nn'}$. The matrix element is now simplified to

$$(M_{if})_{2D} = A_0 \delta_{nn'} \hat{u}_A \bullet M_{CV}(k_{||}, k'_{||}) \tag{4.1-4}$$

where $\hat{u}_A$ is the unit vector along **A**, and

$$M_{CV}(k_{||}, k'_{||}) = \iint \phi^*_{Vk'_{||}}(r_{||})\, p\, \phi_{Ck_{||}}(r_{||})\, d^2r \tag{4.1-5}$$

Substituting (4.1-4) into the expression for transition probability from (3.1-12) and dividing by volume V, we have the transition probability per unit volume as

$$W_{2D} = \frac{2\pi e^2 A_0^2}{\hbar m_c^2 c^2 V} \sum_{k_{||},n} \sum_{k'_{||},n'} \delta_{nn'} \left| \hat{u}_A \bullet M_{CV}(k_{||}, k'_{||}) \right|^2 \left[f_c(E_{Ck_{||}n}) - f_v(E_{Vk'_{||}n'}) \right] \delta\left(E_{Vk'_{||}n'} - E_{Ck_{||}n} + \hbar\omega \right) \tag{4.1-6}$$

Once more, we assume that we are dealing with wave vectors very close to zero, and hence consider $|\mathbf{u}_A \cdot \mathbf{M}_{CV}(\mathbf{k}_{\|},\mathbf{k}_{\|}')|^2 \approx |\mathbf{u}_A \cdot \mathbf{M}_{CV}(0,0)|^2$ to be approximately constant. Taking it outside the summation sign, we use (3.2.1-2) to write the probability in terms of the dipole moment operator μ. Summing over n' with $\delta_{nn'}$, the above is further simplified to

$$W_{2D} = \frac{2\pi\omega^2\mu^2 A_0^2}{\hbar c^2 V} \sum_{k_{\|},n} \sum_{k_{\|}'} \left[f_c(E_{Ck_{\|}n}) - f_v(E_{Vk_{\|}'n}) \right] \delta(E_{Vk_{\|}'n} - E_{Ck_{\|}n} + \hbar\omega) \tag{4.1-7}$$

Following the method in Section 3.1.1, we convert the $\mathbf{k}_{\|}$ and $\mathbf{k}_{\|}'$ summations to integrals extending over the first Brillouin zone and add a factor of 2 for electron spin. Thus, we have

$$W_{2D} = \frac{2\pi\omega^2\mu^2 A_0^2}{\hbar c^2} \sum_n \frac{2A_{\|}}{V} \iint_{BZ} \frac{d^2k_{\|}}{(2\pi)^2} A_{\|} \iint_{BZ} \frac{d^2k_{\|}'}{(2\pi)^2} \left[f_c(E_{Ck_{\|}n}) - f_v(E_{Vk_{\|}'n}) \right] \delta(E_{Vk_{\|}'n} - E_{Ck_{\|}n} + \hbar\omega) \tag{4.1-8}$$

We may rewrite the above expression in terms of the density of states as

$$W_{2D} = \frac{2\pi\omega^2\mu^2 A_0^2}{\hbar c^2 V}\sum_n 2\int_{E_{cn}}^{\infty} dE_{Ck_{\|}n}\rho_c(E_{Ck_{\|}n})\int_{E_{vn}+E_g}^{\infty} dE_{Vk'_{\|}n}\rho_v(E_{Vk'_{\|}n})$$
$$\left[f_c(E_{Ck_{\|}n}) - f_v(E_{Vk'_{\|}n})\right]\delta(E_{Vk'_{\|}n} - E_{Ck_{\|}n} + \hbar\omega) \qquad (4.1\text{-}9)$$

where

$$\rho_c(E_{Ck_{\|}n}) = \frac{A_{\|}}{2}\frac{m_c}{\pi\hbar^2} \qquad (4.1\text{-}10a)$$

$$\rho_v(E_{Vk'_{\|}n}) = \frac{A_{\|}}{2}\frac{m_v}{\pi\hbar^2} \qquad (4.1\text{-}10b)$$

are simply the 2D densities of states for the CB and VB for the volume V, respectively. Upon performing the integrations using the δ-function to set integration limits, we obtain

$$W_{2D} = \frac{\omega^2\mu^2 A_0^2 A_{\|} m_c m_v kT}{\pi c^2\hbar^5 L_z}\sum_n\left[\ln\left(\frac{T_1T_2}{T_3T_4}\right)\right] \qquad (4.1\text{-}11)$$

where

$$T_1 = 1 + \exp\left[\frac{E'_{fv} - E_{vn}}{kT}\right]$$

$$T_2 = 1 + \exp\left[\frac{E_{cn} - E_{fc}}{kT}\right]$$

$$T_3 = 1 + \exp\left[\frac{\hbar\omega - E_g - E_{vn} - E_{fc}}{kT}\right]$$

$$T_4 = 1 + \exp\left[\frac{-\hbar\omega + E_g + E_{cn} + E'_{fv}}{kT}\right]$$

and E_{cn}, E_{vn}, E_{fc}, and E_g are defined in Chapters 2 and 3. E'_{fv} is the Fermi energy for holes in the VB, measured positive downwards from the top of the VB. The 2D gain coefficient per unit volume for the no k-conservation QW case is simply written by substituting W_{2D} from (4.1-11) into expression (3.2-3), as

$$\gamma_{2D}(\omega) = \frac{4\mu^2 A_{||} m_c m_v kT}{\lambda \varepsilon_0 n_r \hbar^4 L_z} \sum_n \left[\ln \left(\frac{T_1 T_2}{T_3 T_4} \right) \right] \qquad (4.1\text{-}12)$$

where we substituted wavelength λ for frequency ω in the constant term outside the summation sign. As in Chapter 3, this gain expression contains no losses. At ordinary concentrations ($N_0 \sim 10^{16} cm^{-3}$), the quasi-Fermi energy levels in each band are low enough to contain only the first few energy quantum levels (E_{cn} and E_{vn}). A Fortran program (listed in Appendix C) was written for calculations. As predicted, for larger concentrations, the optical gain increases, as seen in Figure 4-2. We note a difference in this curve with the corresponding curve in the k-selection situation. The gain curves here show distinct smooth maxima and larger bandwidths, as opposed to the fairly sharp peaks in the previous case.

The next graph {Figure 4-3} depicts the variation of maximum optical gain with carrier concentration. This also differs in shape from its corresponding curve in the case with momentum conserved.

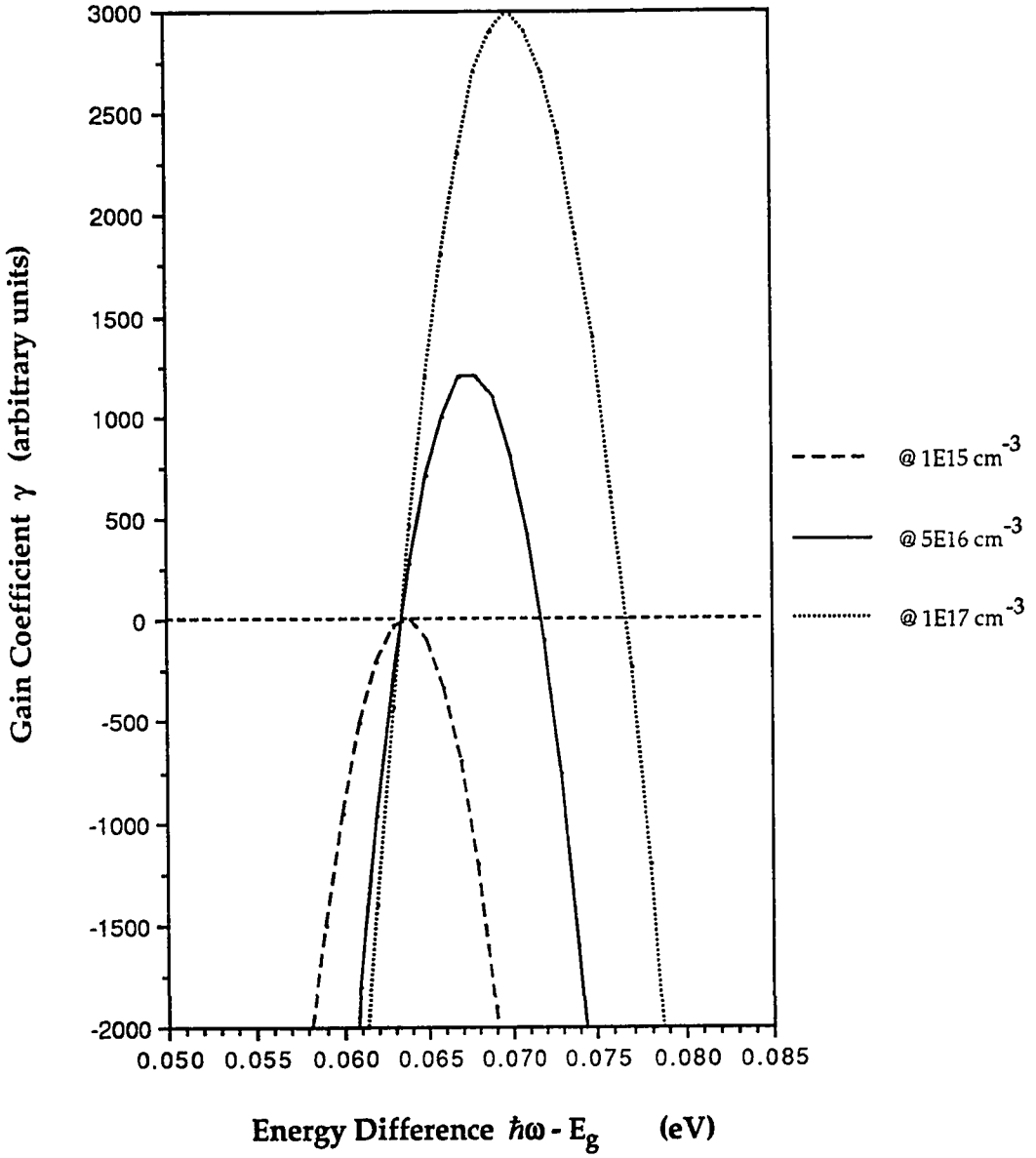

Figure 4-2: Optical gain coefficient per unit volume of a 2D QW structure plotted versus net transition energy at fixed temperature (T = 300 K) and well width (L_z = 100 Å) for various carrier concentrations N_0. The k-selection rule is not obeyed here.

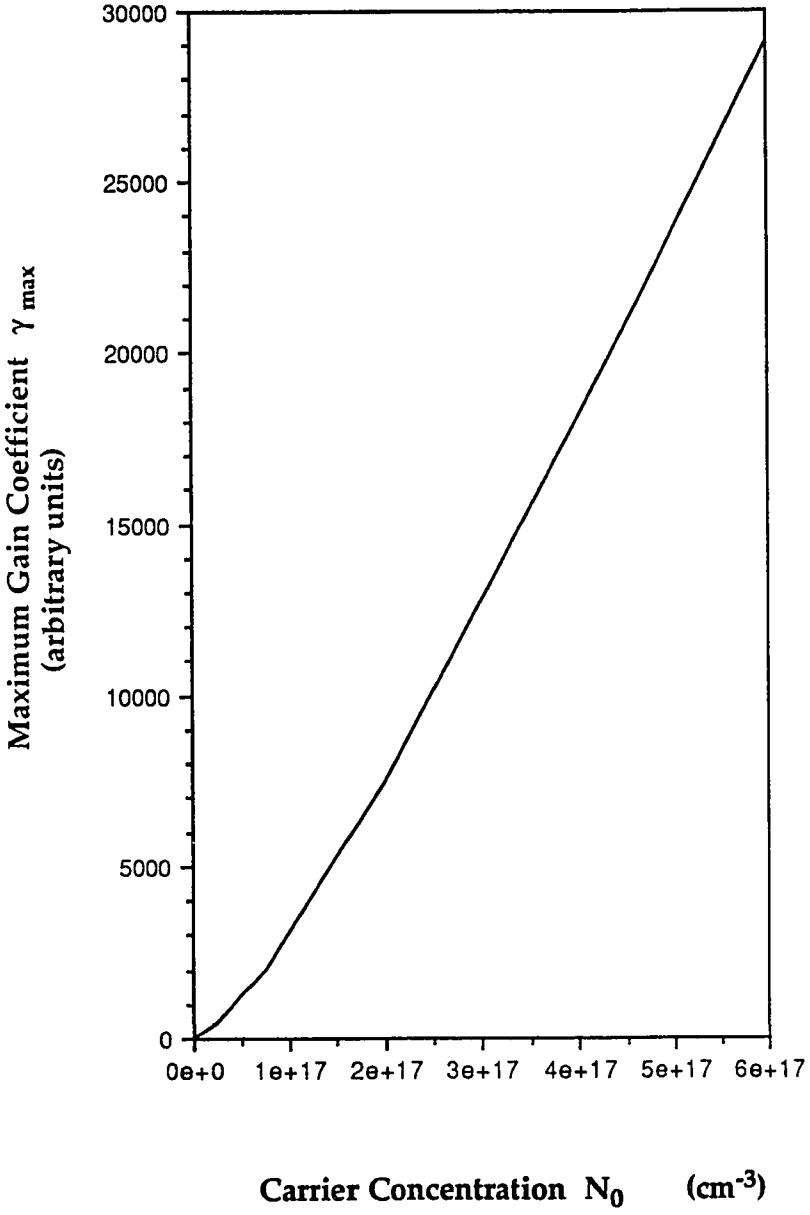

Figure 4-3: Maximum optical gain coefficient per unit volume for a 2D QW structure plotted versus carrier concentration N_0 at fixed temperature (T = 300 K) and well width (L_z = 100 Å). The k-selection rule is not obeyed here.

The third graph (Figure 4-4) shows that optical gain increases with decreasing temperature T, even though from equation (4.1-12), it appears that gain is directly proportional to T, and should hence decrease with T. This apparent paradox is explained as follows. We note that for very low temperatures (in the limit $T \rightarrow 0$), the terms T_1 and T_3 reduce to unity, while T_2 and T_4 reduce to

$$\lim_{kT \rightarrow 0} T_2 = \exp\left[\frac{E_{cn} - E_{fc}}{kT}\right]$$

$$\lim_{kT \rightarrow 0} T_4 = \exp\left[\frac{-\hbar\omega + E_g + E_{cn} + E'_{fv}}{kT}\right]$$

Hence, the gain coefficient reduces to

$$\lim_{kT \rightarrow 0} \gamma_{2D}(\omega) = \frac{4\mu^2 A_{||} m_c m_v}{\lambda \varepsilon_0 n_r \hbar^4 L_z} \left[\hbar\omega - E_g - E_{fc} - E'_{fv}\right] \sum_n 1$$

which is non-zero.

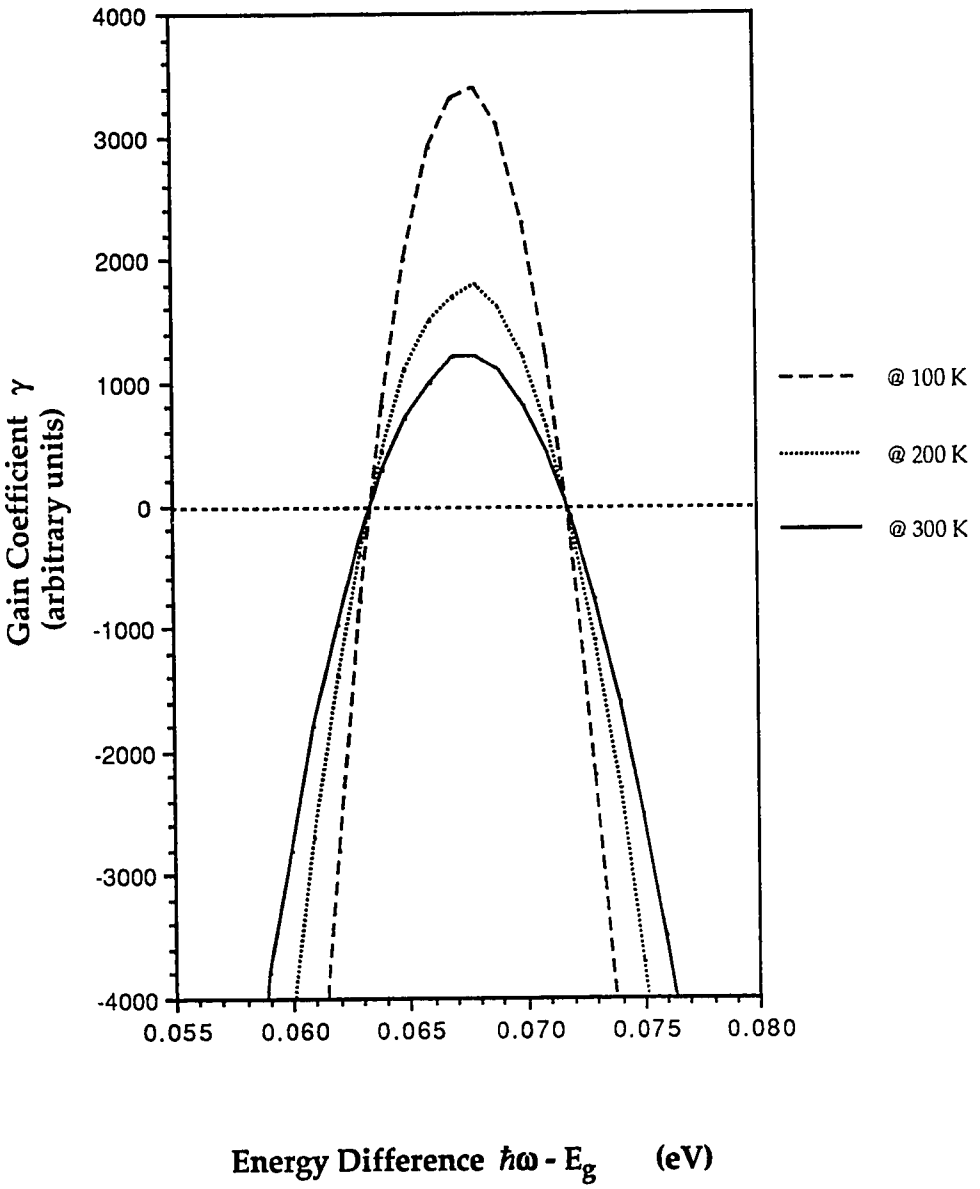

Figure 4-4: Optical gain coefficient per unit volume of a 2D QW structure plotted versus net transition energy at fixed carrier concentration (N_0 = 5E16 cm^{-3}) and well width (L_z = 100 Å) for various temperatures T. The k-selection rule is not obeyed here.

4.2 The One-dimensional Laser System

Following an argument as in Section 4.1, the electron and hole wavefunctions are chosen as

$$\Psi_{Ck_x mn}(x, y, z) = \frac{2}{\sqrt{L_y L_z}} \phi_{Ck_x}(x)\, CS\left(\frac{m\pi}{L_y} y\right) CS\left(\frac{n\pi}{L_z} z\right) \tag{4.2.1a}$$

$$\Psi_{Vk'_x m'n'}(x, y, z) = \frac{2}{\sqrt{L_y L_z}} \phi_{Vk'_x}(x)\, CS\left(\frac{m'\pi}{L_y} y\right) CS\left(\frac{n'\pi}{L_z} z\right) \tag{4.2.1b}$$

where

$$\phi_{Ck_x}(x) = \sum_{k_x} a_{k_x} u_{Ck_x}(x)\, e^{ik_x x} \tag{4.2.2a}$$

$$\phi_{Vk'_x}(x) = \sum_{k'_x} a_{k'_x} u_{Vk'_x}(x)\, e^{ik'_x x} \tag{4.2.2b}$$

are normalized. Starting with the matrix element expression (3.1.2-2), we have

$$\begin{aligned}(M_{if})_{1D} &= \left\langle \Psi_{Vk'_x m'n'} \middle| e^{i\mathbf{q}\cdot\mathbf{r}} A_0 \cdot \mathbf{p} \middle| \Psi_{Ck_x mn} \right\rangle \\ &= \frac{4}{L_y L_z} \iiint \phi^*_{Vk'_x}(x)\, CS\left(\frac{m'\pi}{L_y} y\right) CS\left(\frac{n'\pi}{L_z} z\right) \\ &\qquad e^{i\mathbf{q}\cdot\mathbf{r}} A_0 \cdot \mathbf{p}\, \phi_{Ck_x}(x)\, CS\left(\frac{m\pi}{L_y} y\right) CS\left(\frac{n\pi}{L_z} z\right) d^3 r\end{aligned} \tag{4.2.3}$$

Once more, we assume that $e^{iq\bullet r} \approx 1$, and transitions occur only between bands of same quantum number. We thus obtain the Kronecker δ-functions $\delta_{mm'}$ and $\delta_{nn'}$, and the matrix element is now simplified to

$$(M_{if})_{1D} = A_0 \delta_{mm'} \delta_{nn'} \hat{u}_A \bullet M_{CV}(k_x, k'_x) \qquad (4.2.4)$$

where

$$M_{CV}(k_x, k'_x) = \hat{x} \int \phi^*_{Vk'_x}(x)\, p_x\, \phi_{Ck_x}(x)\, dx \qquad (4.2.5)$$

Substituting (4.2-4) into the expression for transition probability from (3.1-12) and dividing by volume V, we obtain the transition probability per unit volume as

$$W_{1D} = \frac{2\pi\omega^2\mu^2 A_0^2}{\hbar c^2 V} \sum_{k_x,m,n} \sum_{k'_x,m',n'} \delta_{mm'} \delta_{nn'} \left[f_c(E_{Ck_x mn}) - f_v(E_{Vk'_x mn}) \right] \delta\left(E_{Vk'_x mn} - E_{Ck_x mn} + \hbar\omega \right) \qquad (4.2\text{-}6)$$

where μ is the dipole moment operator, obtained as before. Summing over m' and n' with $\delta_{mm'}$ and $\delta_{nn'}$, (4.2-6) is further simplified to

$$W_{1D} = \frac{2\pi\omega^2\mu^2 A_0^2}{\hbar c^2 V} \sum_{m,n} \sum_{k_x} \sum_{k_x'} \left[f_c(E_{Ck_x mn}) - f_v(E_{Vk_x' mn}) \right] \delta (E_{Vk_x' mn} - E_{Ck_x mn} + \hbar\omega) \tag{4.2-7}$$

Following the method in Section 4.1, we convert the k_x and k_x' summations to integrals extending over the first Brillouin zone and add a factor of 2 for electron spin. Thus, we have

$$W_{1D} = \frac{4\pi\omega^2\mu^2 A_0^2}{\hbar c^2 V} \sum_{m,n} 2L_x \int_0^\infty \frac{dk_x}{2\pi} \quad 2L_x \int_0^\infty \frac{dk_x'}{2\pi} \left[f_c(E_{Ck_x mn}) - f_v(E_{Vk_x' mn}) \right] \delta (E_{Vk_x' mn} - E_{Ck_x mn} + \hbar\omega) \tag{4.2-8}$$

Rewriting the above expression in terms of densities of states, we have

$$W_{1D} = \frac{4\pi\omega^2\mu^2 A_0^2}{\hbar c^2 V} \sum_{m,n} \int_{E_{cmn}}^\infty dE_{Ck_x mn} \rho_c(E_{Ck_x mn}) \int_{E_{vmn}+E_g}^\infty dE_{Vk_x' mn} \rho_v(E_{Vk_x' mn}) \left[f_c(E_{Ck_x mn}) - f_v(E_{Vk_x' mn}) \right] \delta (E_{Vk_x' mn} - E_{Ck_x mn} + \hbar\omega) \tag{4.2-9}$$

where

$$\rho_c(E_{Ck_x mn}) = \frac{L_x}{\pi}\sqrt{\frac{m_c}{2\hbar^2}}\left(E_{Ck_x mn} - E_{cmn}\right)^{-\frac{1}{2}} \tag{4.2-10a}$$

$$\rho_v(E_{Vk_x' mn}) = \frac{L_x}{\pi}\sqrt{\frac{m_v}{2\hbar^2}}\left(-E_{Vk_x' mn} - E_{vmn} - E_g\right)^{-\frac{1}{2}} \tag{4.2-10b}$$

are the simple linear (1D) densities of states for the CB and VB, respectively, and E_{cmn},E_{vmn}, and E_g are as defined previously. To solve (4.2-9), we perform the k_x'-integration first using the δ-function to set integration limits. This gives

$$W_{1D} = \frac{4\pi\omega^2\mu^2 A_0^2}{\hbar c^2 V}\sum_{m,n}\int_{E_{cmn}}^{\infty} dE_{Ck_x mn}\rho_c(E_{Ck_x mn})\rho_v(E_{Ck_x mn} - \hbar\omega)$$
$$\left[f_c(E_{Ck_x mn}) - f_v(E_{Ck_x mn} - \hbar\omega)\right] H(\hbar\omega - E_{Ck_x mn} - E_{vmn} - E_g) \tag{4.2-11}$$

Now, the 1D QW gain per unit volume for the no k-conservation case is simply written by substituting W_{1D} from (4.2-11) into expression (3.2-3), as

$$\gamma_{1D}(\omega) = \frac{8\pi^2\mu^2}{\lambda\varepsilon_0 n_r V}\sum_{m,n}\int_{E_{cmn}}^{\infty} dE_{Ck_x mn}\rho_c(E_{Ck_x mn})\rho_v(E_{Ck_x mn} - \hbar\omega)$$
$$\left[f_c(E_{Ck_x mn}) - f_v(E_{Ck_x mn} - \hbar\omega)\right] H(\hbar\omega - E_{Ck_x mn} - E_{vmn} - E_g) \tag{4.2-12}$$

To perform the above integration, we first simplify the integrand by introducing the variable

$$t = \left[\hbar\omega - E_{Ck_x mn} - E_{vmn} - E_g \right]^{\frac{1}{2}}$$

and obtain

$$\gamma_{1D}(\omega) = \frac{16\mu^2 L_x \sqrt{m_c m_v}}{\lambda \varepsilon_0 n_r \hbar^2 L_y L_z} \sum_{m,n} \int_0^{\sqrt{\hbar\omega - E_{rmn} - E_g}} dt \left[\hbar\omega - E_{rmn} - E_g - t^2 \right]^{-\frac{1}{2}}$$
$$\left[f_c(\hbar\omega - E_{vmn} - E_g - t^2) - f_v(-E_{vmn} - E_g - t^2) \right] H(t^2)$$

(4.2-13)

We need to solve the integral in (4.2-13) numerically to obtain gain coefficient values. For this purpose, a Fortran program was written (refer to Appendix D).

Figure 4-5 shows a plot of the no k-selection 1D optical gain coefficient versus energy difference at various carrier concentrations. The gain shows a saturation (maximum value) at higher energy differences, until the difference is large enough to include the next quantum levels. At this point, the gain jumps discontinuously to a higher value. The region of operation for a laser is generally near threshold, so the higher levels are not an important consideration in practice.

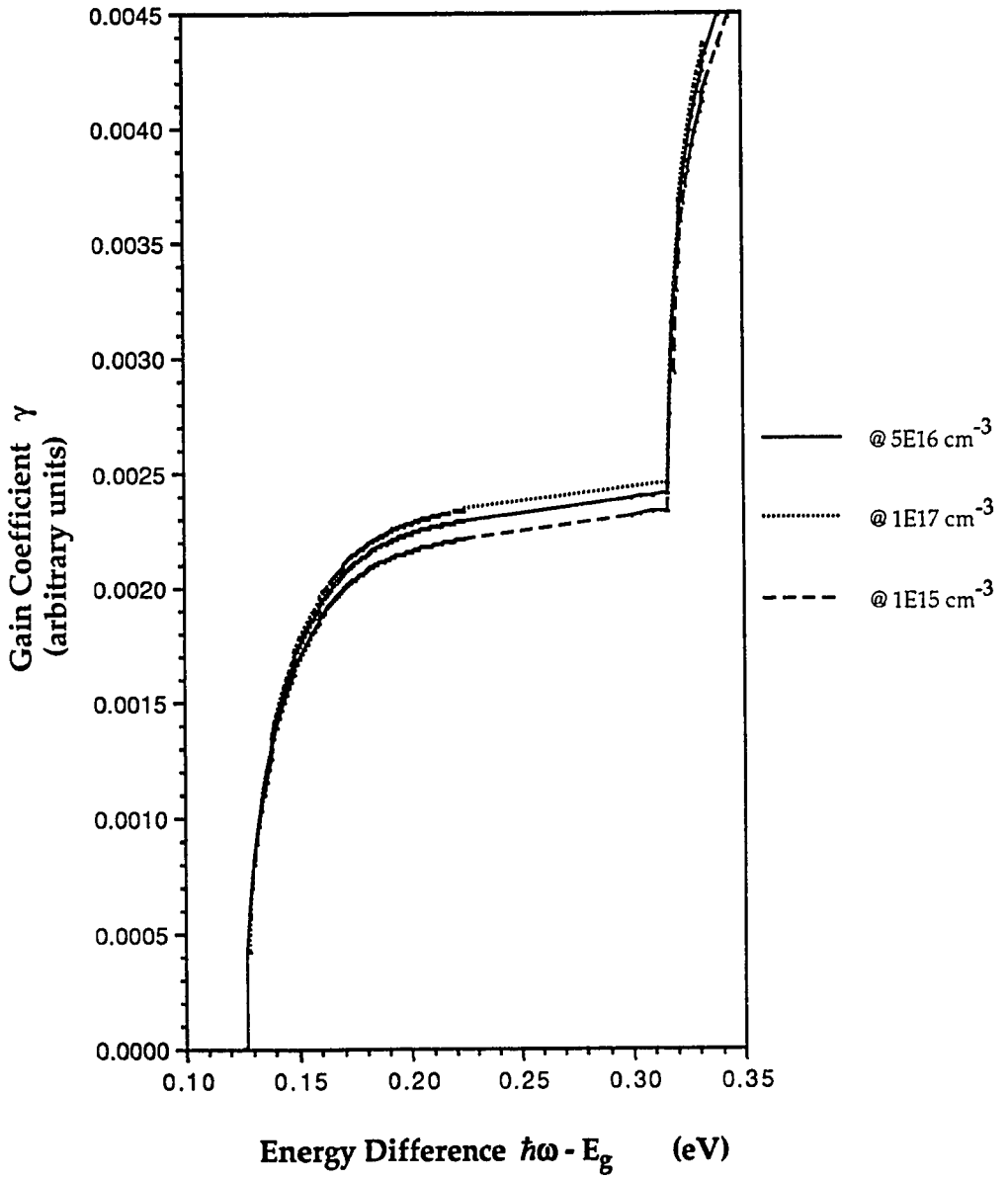

Figure 4-5: Optical gain coefficient per unit volume of a 1D QW structure plotted versus net transition energy at fixed temperature (T = 300 K) and well widths ($L_y = L_z = 100$ Å) for various carrier concentrations N_0. Here, the k-selection rule is not obeyed.

The next figure (Figure 4-6) shows a variation of the maximum optical gain with carrier concentration N_0. The shape of this curve is similar to the variation of maximum gain with N_0 in the k-selection case.

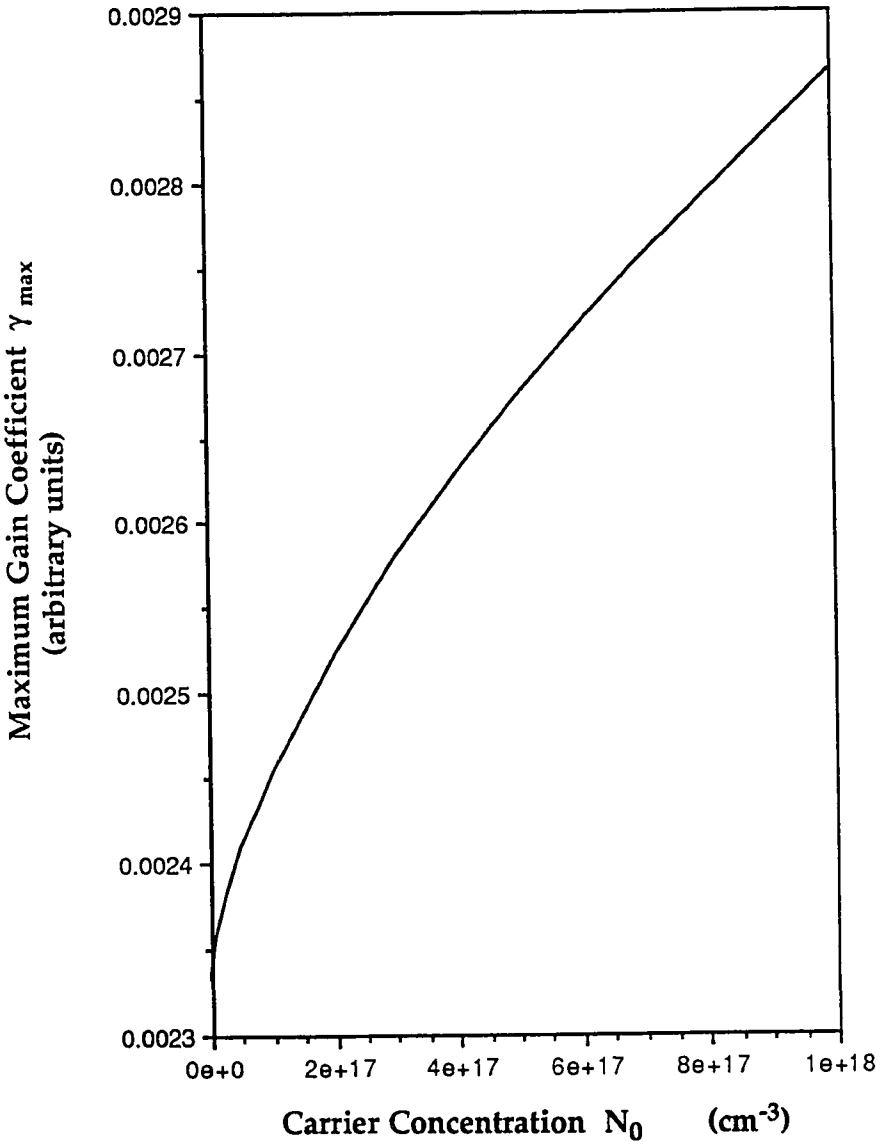

Figure 4-6: Maximum optical gain coefficient per unit volume for a 1D QW structure plotted versus carrier concentration N_0 at fixed temperature (T = 300 K) and well widths ($L_y = L_z$ = 100 Å). The k-selection rule is not obeyed here.

CHAPTER 5: CONCLUSION

In the preceding chapters, we have studied the optical gain in 2D and 1D QW lasers, with and without the k-selection rule. Here, we summarize the observations made and inferences arrived at in our studies.

Firstly, the optical gain of the QW structure increases by reducing the laser dimension along an additional direction. Theoretically, we showed that the ratio of the respective optical gain coefficients is equal to the ratio of the corresponding densities of states. These ratios (2D versus 3D, and 1D versus 2D) are very large near corresponding threshold frequencies of the lasers due to quantization of the structures. This important feature points out the higher overall efficiency of a 2D laser as compared to a 3D, and of the 1D laser as compared to the 2D laser.

Secondly, the ratio of the 1D gain coefficient with the 2D gain coefficient is inversely proportional to the well width along the additional quantized direction in the 1D laser. This observation bears the following implication. The smaller this well width, the larger is the 1D gain as compared to the 2D gain. The peaked nature of the 1D density of states is responsible for a much higher gain in the structure than in a 2D case. This nature is also responsible for a lower temperature dependence of the threshold. The charge carriers near threshold (thus around the peak) have a

very small probability of non-radiative losses by thermal motion, and so are not as strongly affected as in the 2D and bulk cases.

In plotting the maximum gain obtained at various concentrations, we also observe a much lower threshold for the 2D laser ($@N_0 = 4.5x10^{15}$ cm^{-3}) as compared to a 3D laser. The 1D laser shows an even lower threshold current density ($@N_0 = 2.5x10^{15}$ cm^{-3}) . The first obtained stimulated emission from a Quantum Wire laser[36] was followed closely by the lowest recorded threshold current of 3.5mA[37]. Most recently obtained threshold currents are in the μA range {refer to OSA Annual Meeting Technical Digest, Nov, 1991}.

Comparison of similar expressions in the cases with k-selection (momentum conserved) versus those with no k-selection (momentum not conserved) shows higher gain values in the latter. Physically, we argue this point by the fact that the probability of electronic transitions is much greater when the strict momentum conservation rule is laxed. "Non-vertical" transitions may occur along with "vertical" ones, and there is an additional integration over all initial states and final states. However, the overall conclusions about 2D versus 1D QW lasers in the no k-selection case are the same as in the case with k-selection. Optical gain is larger, and threshold is lower in the lower dimensional structures.

Features of higher gain and lower threshold are of major importance for monolithic integration with electronics. Optoelectronic applications such as optical computers and optical communication require ultrafast speed and

low loss components with low operating injection currents (to prevent overheating and melting). The above features imply reduced external losses of optical energy in the integrated circuits, and hence much higher efficiency.

We have used certain approximations such as constant well width[38], and bulk effective mass of carriers[39]. Resonant tunnelling and stimulated phonon emission[40] also takes place. These can be taken into consideration in future studies. Continued in-depth studies of lower dimensional QW lasers (1D, and even zero-D) will greatly contribute to advances in optoelectronic research and technology.

BIBLIOGRAPHY

1. A.L. Schawlow and C.H. Townes, "Infrared and Optical Masers", Phys.Rev., **112**, 1940, (1958).

2. T.H. Maiman, "Stimulated Optical Radiation in Ruby Masers", Nature, **187**, 493, (1960).

3. M.I. Nathan,W.P. Dumke, G. Burns, F.H. Dills, and G. Lasher, "Stimulated Emission of Radiation from GaAs p-n Junctions", App.Phys.Lett., **1**, 62, (1962).

4. R.N. Hall, G.E. Fenner, J.D. Kingsley, T.J. Soltys, and R.O Carlson, "Coherent Light Emission from GaAs Junctions", Phys.Rev.Lett., **9**, 336, (1962).

5. T.M. Quish, R.J. Keyes, W.E. Krag, B. Lax, A.L. McWhorter, R.H. Redike, and H.J. Zeiger, "Semiconductor Maser of GaAs", App.Phys.Lett., **1**, 91, (1962).

6. A. Yariv, "Optical Electronics", 3rd Ed.(New York: Holt, 1985).

7. J. Verdeyen, "Laser Electronics", 2nd Ed.(New Jersey: Prentice-Hall, 1981).

8. J.Wilson and J.F.B.Hawkes, "Optoelectronics: an Introduction", 2nd Ed. (Cambridge, UK: Prentice-Hall, 1989).

9. A.E. Siegman, "Lasers", (Mill Valley, CA: University Science Books, 1986).

10. Leo Esaki, "A Bird's Eye View on the Evolution of Semiconductor Superlattices and Quantum Wells", IEEE J. Quantum Electron., **QE-22**, 1611, (1986).

11. N. Holonyak Jr., R.M. Kolbas, R.D. Dupuis, and P.D. Dapkus, " Quantum Well Heterostructure Lasers", IEEE J. Quantum Electron., **QE-16**, 170, (1980).

12. M.A. Haase, J. Qiu, J.M. DePuydt, and H. Cheng, "Blue-Green II-VI Laser Diodes", Symposium on Lasers, OSA Annual Meeting, (Nov 5, 1991).

13. A. Yariv, "Quantum Electronics", 3rd Ed.(New York: Wiley, 1989).

14. D.L. Crawford, R.L. Nagarajan, and J.E. Bowers, "Comparison of Bulk and Quantum Wire Photodetectors", Appl.Phys.Lett., **58**, 1629, (1991).

15. B. Saint-Cricq, F.Lozes-Dupuy, and G.Vassilieff, "Well Width Dependence of Gain and Threshold Current in GaAlAs Single Quantum Well Lasers ", IEEE J. Quantum Electron., **QE-22**, 625, (1986).

16. Y.Arakawa and A.Yariv, "Quantum Well Lasers-Gain, Spectra, Dynamics" IEEE J. Quantum Electron., **QE-22**, 1887, (1986).

17. Y. Arakawa, K. Vahala, and A. Yariv, "Quantum Noise and Dynamics in Quantum Well and Quantum Wire Lasers", Appl.Phys.Lett., **45**, 1950, (1984).

18. Y. Arakawa and A. Yariv, " Theory of Gain, Modulation Response, and Spectral Linewidth in AlGaAs Quantum Well Lasers", IEEE J. Quantum Electron., **QE-21**, 1666, (1985).

19. J.L. Jewell, K.F. Huang, Y.H. Lee, R.J. Fischer, S.L. McCall, and A.Y. Cho, "Vertical Cavity Single Quantum Well Laser", Appl.Phys.Lett., **55**, 424, (1989).

20. Y. Arakawa and H. Sakaki, " Multidimensional Quantum Well Laser and Temperature Dependence of its Threshold Current", Appl.Phys.Lett., **40**, 939, (1982).

21. A. Sugimura, " Threshold Currents for AlGaAs Quantum Well Lasers", IEEE J. Quantum Electron., **QE-20**, 336, (1984).

22. N. Holonyak,Jr. and B. A. Vojak, "Temperature Dependence of Threshold Current for Quantum-Well $Al_xGa_{1-x}As$-GaAs Heterostructure Laser Diodes", Appl.Phys.Lett., **36**, 19, (1980).

23. N.K. Dutta, "Calculated Threshold Current of GaAs Quantum Well Lasers", J.Appl.Phys., **53**, 7211, (1982).

24. D. Gershoni, H. Temkin, G.J. Dolan, J. Dunsmuir, S.N.G. Chu, and M.B. Panish, "Effects of Two-dimensional Confinement on the Optical Properties of InGaAs/InP Quantum Wire Structures", Appl.Phys.Lett., **53**, 995, (1988).

25. H. Sakaki, K. Kato, and H. Yoshimura, "Optical Absorption and Carrier-induced Bleaching Effect in Quantum Wire and Quantum Box Structures", Appl.Phys.Lett., **57**, 2800, (1990).

26. L.I. Schiff, "Quantum Mechanics", 3rd Ed.(New York: McGraw-Hill, 1968).

27. J.D. Jackson, "Classical Electrodynamics", 2nd Ed.(New York: Wiley, 1975).

28. F. Bassani and G.P. Parravicini, "Electronic States and Optical Transitions in Solids", (Oxford: Pergamon Press, 1975).

29. N. Holonyak,Jr. et al, "Phonon-assisted Recombination and Stimulated Emission in Quantum Well $Al_xGa_{1-x}As$-GaAs Heterostructure", J.Appl.Phys., **51**, 1332, (1980).

30. T. Takahashi and Y. Arakawa, "Nonlinear Gain Effects in Quantum Well, Quantum Well Wire, and Quantum Well Bow Lasers", IEEE J.Quantum Electron., **27**, 1824, (1991).

31. C. Kittel, "Introduction to Solid State Physics", 5th Ed.(New York: Wiley, 1985).

32. G. Burns, "Solid State Physics", (New York: Academic Press, 1985).

33. G. Lasher and F. Stern, "Spontaneous and Stimulated Recombination Radiation in Semiconductors", Phys.Rev., **133**, A553, (1964).

34. P.T. Landsberg, M.S. Abrahams, and M. Osinski, "Evidence of No k-Selection in Gain Spectra of Quantum Well AlGaAs Laser Diodes", IEEE J.Quantum Electron., **21**, 24, (1985).

35. W.H. Press, B.P. Flannery, S.A. Teukolsky, and W.T.Vettering, "Numerical Recipies: The Art of Scientific Computing (Fortran Version)", (Cambridge, UK: Cambridge University Press, 1989).

36. E. Kapon, D.M. Hwang, and R. Bhat, "Stimulated Emission in Semiconductor Quantum Wire Heterostructures", Phys.Rev.Lett., **63**, 430, (1989).

37. E. Kapon, S. Simhony, R. Bhat, and D.M. Hwang, "Single Quantum Wire Lasers", Appl.Phys.Lett., **55**, 2715, (1989).

38. R Lang and K. Nishi, "Electronic State Localization in Semiconductor Superlattices", Appl.Phys.Lett., **45**, 98, (1984).

39. K. Suemune and Coldren, "GaAs Quantum Wire Structures", IEEE J. Quantum Electron., **24**, 1784, (1988).

40. S. Briggs, D. Jovanic, and J.P. Leburton, "Intersubband Population Inversion in Quantum Wire Structures", Appl.Phys.Lett., **54**, 2012, (1989).

APPENDIX A

```
************************************************************************
*       CALCULATION OF GAIN COEFFICIENT GAM FOR 2-D QUANTUM WELL:
*       WITH k-SELECTION CASE.
*       This is the most general program for calculation of GAM. Programs in which gain
*       is varied with various parameters are modified versions of this program, where
*       each parameter is input externally. Most of the variables coincide with their
*       counterparts in the gain coefficient expression calculated. Ph = photon energy ħω,
*       and others are defined at places where they appear.
************************************************************************

 100   DIMENSION Ph(100),PhEgc(100),PhEgv(100),
     &       Fc(100),Fv(100),RHO(100),GAM(100)
       REAL  Eg,En,B,INPh,No,Ph,PhEgc,PhEgv,LZ,CONc,CONv,H,RHO,S,
     &    T,kT,Fc,Fv,Efc,Efco,Efv,Efvo,GAM,GAMCON,Ec1,Ev1,PI2
       INTEGER I,K,M,N,ANS,ANSW
       PARAMETER (CONc=552.915,CONv=81.7351,PI2=0.82247,Eg = 1.45)

*      CONc = (hbar**2/2mc#)*pi**2, in units of eV-ANG**2 for electrons
*      CONv = (hbar**2/2mv#)*pi**2, in units of eV-ANG**2 for holes
*      PI2  = pi**2/12

       OPEN (5,FILE='QW2GAINDAT',STATUS='NEW')
       WRITE(9,1) 'ENTER INITIAL ENERGY OF PHOTON IN eV'
 1     FORMAT(/,1X,A48)
       READ*, INPh
       WRITE(9,1) 'ENTER NUMBER OF ENERGY VALUES REQUIRED'
       READ*, M
       WRITE(9,1) 'ENTER INCREMENT OF ABOVE ENERGY'
       READ*, S
       WRITE(9,1) 'UPPER LIMIT FOR SUMMATION OF ENERGY STATES'
       READ*, N
       WRITE(9,1) 'ENTER CARRIER CONCENTRATION IN cm3'
       READ*, No
       WRITE(9,1) 'ENTER TEMPERATURE IN KELVIN'
       READ*, T
       WRITE(9,1) 'ENTER WELL WIDTH IN ANGSTROM'
       READ*, LZ

       WRITE(9,2) 'TEMPERATURE T = ',T,'K','WELL WIDTH LZ = ',LZ,
     &      'ANG','CONCENTRATION No =',No,'cm-3'
       WRITE(5,2) 'TEMPERATURE T = ',T,'K','WELL WIDTH LZ = ',LZ,
     &      'ANG','CONCENTRATION No =',No,'cm-3'
 2     FORMAT(1X,A19,F5.1,A2,/,A19,F5.1,A3,/,A19,E7.2,A4)
```

```
      WRITE(9,3) 'PHOTON ENERGY RANGE (eV):',INPh,'TO',INPh+M*S
      WRITE(5,3) 'PHOTON ENERGY RANGE (eV):',INPh,'TO',INPh+M*S
3     FORMAT(/,1X,A31,2X,F5.3,2X,A2,2X,F5.3,/)

      WRITE(9,1) 'CONTINUE (Y=any key/N=0)?'
      READ*, ANS
      IF (ANS.EQ.0) THEN
      WRITE(9,1) 'GOODBYE'
      GO TO 700
      ELSE
      GO TO 350
      ENDIF

***   Calculation of quasi-Fermi energy levels at temperature T
350   Ec1 = CONc/(LZ**2)
      Ev1 = CONv/(LZ**2)
      kT = T/11600.0
      Efco = 536.174E-16*(No**0.6667)
      Efvo = 79.26E-16*(No**0.6667)
      IF (kT.LT.(Efco/3.)) THEN
            Efc = Efco*(1 - PI2*(kT/Efco)**2) + Ec1
      ELSE
            Efc = Efco + Ec1
      ENDIF

      IF (kT.LT.(Efvo/3.)) THEN
            Efv = Efvo*(1 - PI2*(kT/Efvo)**2) + Ev1
      ELSE
            Efv = Efvo + Ev1
      ENDIF

      WRITE(5,4)  'kT=',kT,'Efco=',Efco,'Efvo=',Efvo,
     &            'Efc=',Efc,'Efv=',Efv
4     FORMAT(/,1X,A3,T4,F7.5,T12,A5,T18,F7.5,T26,A5,T31,F8.5,
     &  /,A4,F7.5,4X,A4,F7.5)

*     kT = in units of eV
*     Efco = (hbar**2/2mc)(3pi**2*No*1E-24)**(2/3) in eV @ 0 K
*     Efvo = (hbar**2/2mv)(3pi**2*No*1E-24)**(2/3) in eV @ 0 K
*     Ec1 = energy in eV of first quantum level in the CB (zero pt. energy)
*     Ev1 = energy in eV of first quantum level in the VB (zero pt. energy)
*     Efc = Efco(1 - (pi**2/12)*(kT/Efco)**2) + Ec1 in eV @ T K
*     Efv = Efvo(1 - (pi**2/12)*(kT/Efvo)**2) + Ev1 in eV @ T K

      DO 10 K = 0,M
        Ph(K) = INPh + K*S
**** Calculation of Fermi functions
        PhEgc(K) = (0.87118*(Ph(K)-Eg) - Efc)/kT
        Fc(K) = 1/(1+EXP(PhEgc(K)))
        PhEgv(K) =(0.12878*Eg-0.12878*Ph(K)+Efv)/kT
        Fv(K) = 1/(1+EXP(PhEgv(K)))
```

```
**** Calculation of Density of States
        RHO(K) = 0.0
        En = 0.0
        B = 0.0
        H = 0.0
**** Summation over quantum number n performed
        DO 20 I = 1,N
             En = Eg + (CONc+CONv)*(I/LZ)**2
             B = Ph(K) - En
             IF (B.LT.0.0001) THEN
               GO TO 10
             ELSE
               H = 1.0
             ENDIF
             RHO(K) = RHO(K) + H
20      CONTINUE
10     CONTINUE

       WRITE(5,5) 'Ph(K)-Eg'
5      FORMAT(/,1X,A12,/)
6      FORMAT(1X,F5.3)
       DO 71 K = 0,M
       WRITE(5,6) Ph(K)-Eg
71     CONTINUE

****   GAMCON = Constant multiple of gain expression for gain in cm-1.
       WRITE(5,5) 'GAM(K)'
8      FORMAT(1X,F11.2)
       DO 73 K = 0,M
       GAMCON=8339.8518*Ph(K)/LZ
       GAM(K) = GAMCON*(Fc(K)-Fv(K))*RHO(K)
       WRITE(5,8) GAM(K)
73     CONTINUE

       WRITE(9,1) 'QUIT= any key / RUN PROGRAM AGAIN = 1 ?'
       WRITE(9,1) 'CAUTION: PREVIOUS DATA WILL BE LOST !'
       READ*, ANSW
       IF (ANSW.EQ.1) THEN
         GO TO 100
         ELSE
         WRITE(9,1) 'GOODBYE !'
         GO TO 700
       ENDIF


700    END
```

APPENDIX B

```
**********************************************************************
*       CALCULATION OF GAIN COEFFICIENT GAM FOR 1-D QUANTUM WELL:
*       WITH k-SELECTION CASE.
*       This is the most general program for calculation of GAM. Programs in which gain
*       is varied with various parameters are modified versions of this program, where
*       each parameter is input externally. Most of the variables coincide with their
*       counterparts in the gain coefficient expression calculated. Ph = photon energy ħω,
*       and others are defined at places where they appear. Gain calculations were made
*       for LY=LZ for simplification, and a small damping factor dp prevents numeric
*       overflow at runtime due to x tending to 0 in the 1/sqrt(x) term.
**********************************************************************

 100    DIMENSION Ph(200),PhEgc(200),PhEgv(200),Fc(200),Fv(200),
    &   RHO(200),GAM(200)
        REAL Eg,En,B,INPh,No,Ph,PhEgc,PhEgv,LY,LZ,CONc,CONv,H,RHO,S,
    &        T,kT,Fc,Fv,Efc,Efco,Efv,Efvo,GAM,GAMCON,NREF,EPS,
    &        Ec1,Ev1,dp
        INTEGER I,K,R,M,N,ANS,ANSW
        PARAMETER (CONc=552.915,CONv=81.7351,PI2=0.82247,dp=0.001,
    &              Eg=1.45)

*       CONc = (hbar**2/2mc#)*pi**2, in units of eV-ANG**2 for electrons
*       CONv = (hbar**2/2mv#)*pi**2, in units of eV-ANG**2 for holes
*       PI2  = pi**2/12
*       dp = damping factor

        OPEN (5,FILE='QW1GAINDAT',STATUS='NEW')
        WRITE(9,1) 'ENTER INITIAL ENERGY OF PHOTON IN eV'
 1      FORMAT(/,1X,A48)
        READ*, INPh
        WRITE(9,1) 'ENTER NUMBER OF ENERGY VALUES REQUIRED'
        READ*, R
        WRITE(9,1) 'ENTER INCREMENT OF ABOVE ENERGY'
        READ*, S
        WRITE(9,1) 'UPPER LIMIT FOR SUMMATION OF EIGENVALUES EY'
        READ*, M
        WRITE(9,1) 'UPPER LIMIT FOR SUMMATION OF EIGENVALUES EZ'
        READ*, N
        WRITE(9,1) 'WELL WIDTHS IN ANGSTROMS ALONG Y-,Z-AXES:LY,LZ ?'
        READ*, LY,LZ
        WRITE(9,1) 'ENTER CARRIER CONCENTRATION IN cm3'
        READ*, No
        WRITE(9,1) 'ENTER TEMPERATURE IN KELVIN'
        READ*, T
```

```
      WRITE(5,2) 'TEMPERATURE T = ',T,'K','WELL WIDTH LY=LZ=',LY,
     &     'ANG','CONCENTRATION No =',No,'cm-3'
2     FORMAT(1X,A19,F5.1,A2,/,A19,F5.1,A3,/,A19,E7.2,A4)

      WRITE(9,3) 'PHOTON ENERGY RANGE (eV):',INPh,'TO',INPh+R*S
      WRITE(5,3) 'PHOTON ENERGY RANGE (eV):',INPh,'TO',INPh+R*S
3     FORMAT(/,1X,A31,2X,F5.3,2X,A2,2X,F5.3,/)

      WRITE(9,1) 'CONTINUE (Y=any key/N=0)?'
      READ*, ANS
      IF (ANS.EQ.0) THEN
            WRITE(9,1) 'GOODBYE'
            GO TO 700
      ELSE
            GO TO 350
      ENDIF

***   Calculation of quasi-Fermi energies at temperature T.
350   Ec1 = CONc*(1/LY**2 + 1/LZ**2)
      Ev1 = CONv*(1/LY**2 + 1/LZ**2)
      kT = T/11600.0
      Efco = 536.174E-16*(No**0.6667)
      Efvo = 79.26E-16*(No**0.6667)
      IF (kT.LT.(Efco/3.)) THEN
            Efc = Efco*(1 - PI2*(kT/Efco)**2) + Ec1
      ELSE
            Efc = Efco + Ec1
      ENDIF
      IF (kT.LT.(Efvo/3.)) THEN
            Efv = Efvo*(1 - PI2*(kT/Efvo)**2) + Ev1
      ELSE
            Efv = Efvo + Ev1
      ENDIF

      WRITE(5,4)  'kT=',kT,'Efco=',Efco,'Efvo=',Efvo,
     &           'Efc=',Efc,'Efv=',Efv
4     FORMAT(/,1X,A3,T4,F7.5,T12,A5,T18,F7.5,T26,A5,T31,F8.5,
     &  /,A4,F7.5,4X,A4,F7.5)

*     kT = in units of eV
*     Efco = (hbar**2/2mc)(3pi**2*No*1E-24)**(2/3) in eV
*     Efvo = (hbar**2/2mv)(3pi**2*No*1E-24)**(2/3) in eV

      DO 10 K = 0,R
        Ph(K) = INPh + K*S
**** Calculation of Fermi functions
        PhEgc(K) = (0.87118*(Ph(K)-Eg) - Efc)/kT
        Fc(K) = 1/(1+EXP(PhEgc(K)))
        PhEgv(K) =(0.12878*Eg-0.12878*Ph(K)+Efv)/kT
        Fv(K) = 1/(1+EXP(PhEgv(K)))
```

```
**** Calculation of Density of States
          RHO(K) = 0.0
          En = 0.0
          B = 0.0
          H = 0.0
          DO 20 I = 1,M
                DO 30 J = 1,N
                  En = Eg + (CONc+CONv)*((I/LY)**2 + (J/LZ)**2)
                  B = Ph(K) - En
                  IF (B.LT.0.0001) THEN
                    GO TO 20
                  ELSE
                    H = SQRT(B/(B**2+dp**2))
                  ENDIF
                  RHO(K) = RHO(K) + H
30              CONTINUE
20        CONTINUE
10      CONTINUE

        WRITE(5,5) 'Ph(K)-Eg'
5       FORMAT(/,1X,A12,/)
6       FORMAT(1X,F6.4)
        DO 71 K = 0,R
        WRITE(5,6) Ph(K)-Eg
71      CONTINUE

        WRITE(5,5) 'GAM(K)'
****    GAMCON = Constant multiple of gain expression giving gain in cm-1.
8       FORMAT(1X,F12.2)
        DO 73 K = 0,R
        GAMCON=133759.059*Ph(K)/(LY*LZ)
        GAM(K) = GAMCON*(Fc(K)-Fv(K))*RHO(K)
        WRITE(5,8) GAM(K)
73      CONTINUE

        WRITE(9,1) 'RUN PROGRAM AGAIN = 1/QUIT = any key ?'
        WRITE(9,1) 'CAUTION: PREVIOUS DATA WILL BE LOST !'
        READ*, ANSW
        IF (ANSW.EQ.1) THEN
        GO TO 100
        ELSE
        WRITE(9,1) 'GOODBYE !'
        GO TO 700
        ENDIF

700     END
```

APPENDIX C

```
************************************************************************
*       CALCULATION OF GAIN COEFFICIENT GAM FOR 2-D QUANTUM WELL:
*       NO k-SELECTION CASE.
*       This is the most general program for calculation of GAM. Programs in which gain
*       is varied with various parameters are modified versions of this program, where
*       each parameter is input externally. Most of the variables coincide with their
*       counterparts in the gain coefficient expression calculated. Ph = photon energy ħω,
*       and others are defined at places where they appear.
************************************************************************

100     DIMENSION Ph(100),LGM(100),LG(100),GAM(100)
        REAL Eg,Ecn,Evn,INPh,No,Ph,LZ,CONc,CONv,S,T,kT,Efc,Efv,
     &          GAM,GAMCON,T1,T2,T3,T4,LGM,LG,PI2,AREA,
     &          LGNUM,LGDEN,Efco,Efvo,Ec1,Ev1
        INTEGER I,K,M,N,ANS,ANSW
        PARAMETER (CONc=552.915,CONv=81.7351,PI2=0.82247,Eg = 1.45)

*       CONc = (hbar**2/2mc)*pi**2, in units of eV-ANG**2 for electrons
*       CONv = (hbar**2/2mv)*pi**2, in units of eV-ANG**2 for holes

        OPEN (5,FILE='NK2GAINDAT',STATUS='NEW')
        WRITE(9,1) 'ENTER INITIAL ENERGY OF PHOTON IN eV'
1       FORMAT(/,1X,A48)
        READ*, INPh
        WRITE(9,1) 'ENTER NUMBER OF ENERGY VALUES REQUIRED'
        READ*, M
        WRITE(9,1) 'ENTER INCREMENT OF ABOVE ENERGY'
        READ*, S
        WRITE(9,1) 'UPPER LIMIT FOR SUMMATION OF ENERGY STATES'
        READ*, N
        WRITE(9,1) 'QW WIDTH LZ IN ANGSTROMS'
        READ*, LZ
        WRITE(9,1) 'AREA (LxLy) OF ACTIVE REGION IN SQ. MICRONS?'
        READ*, AREA
        WRITE(9,1) 'ENTER CARRIER CONCENTRATION IN cm3'
        READ*, No
        WRITE(9,1) 'ENTER TEMPERATURE IN KELVIN'
        READ*, T

        WRITE(5,2) 'TEMPERATURE T = ',T,'K','WELL WIDTH LZ = ',LZ,
     &          'ANG','CONCENTRATION No =',No,'cm-3'
2       FORMAT(1X,A19,F5.1,A2,/,A19,F5.1,A3,/,A19,E7.2,A4)
```

```
      WRITE(9,3) 'PHOTON ENERGY RANGE (eV):',INPh,'TO',INPh+M*S
      WRITE(5,3) 'PHOTON ENERGY RANGE (eV):',INPh,'TO',INPh+M*S
3     FORMAT(/,1X,A31,2X,F5.3,2X,A2,2X,F5.3,/)

      WRITE(9,1) 'CONTINUE (Y=any key/N=0)?'
      READ*, ANS
      IF (ANS.EQ.0) THEN
            WRITE(9,1) 'Goodbye'
            GO TO 700
      ELSE
            GO TO 350
      ENDIF

***   Calculation of quasi-Fermi energies at temperatures T
350   Ec1 = CONc/(LZ**2)
      Ev1 = CONv/(LZ**2)
      kT = T/11600.0
      Efco = 536.174E-16*(No**0.6667)
      Efvo = 79.26E-16*(No**0.6667)
      IF (kT.LT.(Efco/3.)) THEN
            Efc = Efco*(1 - PI2*(kT/Efco)**2) + Ec1
      ELSE
            Efc = Efco + Ec1
      ENDIF
      IF (kT.LT.(Efvo/3.)) THEN
            Efv = Efvo*(1 - PI2*(kT/Efvo)**2) + Ev1
      ELSE
            Efv = Efvo + Ev1
      ENDIF

      WRITE(9,4)  'kT=',kT,'Efco=',Efco,'Efvo=',Efvo,
     &            'Efc=',Efc,'Efv=',Efv
      WRITE(5,4)  'kT=',kT,'Efco=',Efco,'Efvo=',Efvo,
     &            'Efc=',Efc,'Efv=',Efv
4     FORMAT(/,1X,A3,T4,F7.5,T12,A5,T18,F7.5,T26,A5,T31,F8.5,
     &  /,A4,F7.5,4X,A4,F7.5)

*     kT = in units of eV
*     Efco = (hbar**2/2mc)(3pi**2*No*1E-24)**(2/3) in eV @ 0 K
*     Efvo = (hbar**2/2mv)(3pi**2*No*1E-24)**(2/3) in eV @ 0 K
*     Efc = Efco(1 - (pi**2/12)*(kT/Efco)**2) + Ec1 in eV @ T K
*     Efv = Efvo(1 - (pi**2/12)*(kT/Efvo)**2) + Ev1 in eV @ T K

      DO 10 K = 0,M
        Ph(K) = INPh + K*S
**** Calculation of Log functions
        LG(K) = 0.0
        DO 20 I = 1,N
            Ecn = CONc*(I/LZ)**2
            Evn = CONv*(I/LZ)**2
            T1 = LOG(1 + EXP((Efv - Evn)/kT))
```

```
            T2 = LOG(EXP(-Ecn/kT) + EXP(-Efc/kT))
            T3 = LOG(1 + EXP((Ph(K) - Evn - Eg - Efc)/kT))
            T4 = LOG(EXP(-Ecn/kT) + EXP((-Ph(K) + Eg + Efv)/kT))
            LG(K) = LG(K) +T1 + T2 -T3 -T4
20        CONTINUE
10      CONTINUE

        WRITE(5,5) 'Ph(K)-Eg'
5       FORMAT(/,1X,A12,/)
6       FORMAT(1X,F6.4)
        DO 71 K = 0,M
        WRITE(5,6) Ph(K)-Eg
71      CONTINUE

****  GAMCON = Constant multiple of gain for gain in units of 7.92958E8 m-1.
****  Will use arbitrary units for plotting, until actual constant without
****  the AREA is determined.

        WRITE(5,5) 'GAM(K)'
        DO 72 K = 0,M
            GAMCON=T*AREA*Ph(K)/LZ
            GAM(K) = GAMCON*LG(K)
            WRITE(5,7) GAM(K)
7           FORMAT(1X,E12.2)
72      CONTINUE

        WRITE(9,1) 'RUN PROGRAM AGAIN = 1/QUIT = any key'
        WRITE(9,1) 'CAUTION: PREVIOUS DATA WILL BE LOST !'
        READ*, ANSW
        IF (ANSW.EQ.1) THEN
            GO TO 100
        ELSE
            WRITE(9,1) 'GOODBYE !'
            GO TO 700
        ENDIF

700     END
```

APPENDIX D

```
**********************************************************************
*       CALCULATION OF GAIN COEFFICIENT GAMA FOR 1-D QUANTUM WELL
*       NO k-SELECTION CASE.
*       This is the most general program for calculation of GAMA. Programs in which gain
*       is varied with various parameters are modified versions of this program, where
*       each parameter is input externally. The program uses the Gaussian numerical
*       integration subroutine QGAUSS from reference [35]. The function RINGD to be
*       integrated is read externally by QGAUSS. Most of the variables coincide with their
*       counterparts in the gain coefficient expression calculated. PHO = photon energy
*       ħω, and others are defined at places where they appear. A damping factor
*       dp=0.001eV is used to prevent the integrand from becoming a singularity.
**********************************************************************

 100    DIMENSION PHO(200),GAM(200),GAMA(200)
        REAL INPh,Eg,No,LX,LY,LZ,CONc,CONv,T,kT,Efc,Efv,Ermn,
    &   Evmn,PH,PHO,GA,GAM,GAMCON,GAMA,S,AA,BB,BR,Efco,
    &   Efvo,Ec1,Ev1,dp
         INTEGER I,J,K,M,N,R,ANS,ANSW
        PARAMETER (CONc=552.915,CONv=81.7351,PI2=0.82247,
    &         dp=0.001,AA = 0.0,Eg=1.45)
        EXTERNAL RINGD
        COMMON/ATT/Eg,kT,Efc,Efv,Ermn,Evmn,PH

*       CONc = (hbar**2/2mc#)*pi**2, in units of eV-ANG**2 for electrons
*       CONv = (hbar**2/2mv#)*pi**2, in units of eV-ANG**2 for holes

        OPEN (5,FILE='NK1GAINDAT',STATUS='NEW')
        WRITE(9,1) 'ENTER INITIAL ENERGY OF PHOTON IN eV'
 1      FORMAT(/,1X,A48)
        READ*, INPh
        WRITE(9,1) 'ENTER NUMBER OF ENERGY VALUES REQUIRED'
        READ*, R
        WRITE(9,1) 'ENTER INCREMENT OF ABOVE ENERGY'
        READ*, S
        WRITE(9,1) 'ENTER CARRIER CONCENTRATION IN cm3'
        READ*, No
        WRITE(9,1) 'ENTER TEMPERATURE IN KELVIN'
        READ*, T
        WRITE(9,1) 'ENTER DIMENSION LX IN MICRONS'
        READ*, LX
        WRITE(9,1) 'ENTER WELL WIDTHS LY,LZ IN ANGSTROMS'
        READ*, LY,LZ
        WRITE(9,1) 'UPPER LIMIT M FOR SUMMATION OF EIGENVALUES EY'
        READ*, M
        WRITE(9,1) 'UPPER LIMIT N FOR SUMMATION OF EIGENVALUES EZ'
```

```
      WRITE(9,1) 'UPPER LIMIT N FOR SUMMATION OF EIGENVALUES EZ'
      READ*, N
      WRITE(5,2) 'TEMPERATURE T = ',T,'K','WELL WIDTH LY=LZ=',LY,
     &     'ANG','CONCENTRATION No =',No,'cm-3'
2     FORMAT(1X,A19,F5.1,A2,/,A19,F5.1,A3,/,A19,E7.2,A4)

      WRITE(9,3) 'PHOTON ENERGY RANGE (eV):',INPh,'TO',INPh+R*S
      WRITE(5,3) 'PHOTON ENERGY RANGE (eV):',INPh,'TO',INPh+R*S
3     FORMAT(/,1X,A31,2X,F5.3,2X,A2,2X,F5.3,/)

      WRITE(9,1) 'CONTINUE (Y=any key/N=0)?'
      READ*, ANS
      IF (ANS.EQ.0) THEN
            WRITE(9,1) 'Goodbye!'
            GO TO 700
      ELSE
            GO TO 350
      ENDIF

350   kT = T/11600.0
      Ec1 = CONc*(1/LY**2 + 1/LZ**2)
      Ev1 = CONv*(1/LY**2 + 1/LZ**2)
      kT = T/11600.0
      Efco = 536.174E-16*(No**0.6667)
      Efvo = 79.26E-16*(No**0.6667)
      IF (kT.LT.(Efco/3.)) THEN
            Efc = Efco*(1 - PI2*(kT/Efco)**2) + Ec1
      ELSE
            Efc = Efco + Ec1
      ENDIF
      IF (kT.LT.(Efvo/3.)) THEN
            Efv = Efvo*(1 - PI2*(kT/Efvo)**2) + Ev1
      ELSE
            Efv = Efvo + Ev1
      ENDIF

      WRITE(5,4)  'kT=',kT,'Efco=',Efco,'Efvo=',Efvo,
     &      'Efc=',Efc,'Efv=',Efv
4     FORMAT(/,1X,A3,T4,F7.5,T12,A5,T18,F7.5,T26,A5,T31,F8.5,
     &  /,A4,F7.5,4X,A4,F7.5)

*     kT = in units of eV
*     Efco = (hbar**2/2mc)(3pi**2*No*1E-24)**(2/3) in eV @ 0 K
*     Efvo = (hbar**2/2mv)(3pi**2*No*1E-24)**(2/3) in eV @ 0 K
*     Ec1 = energy in eV of first quantum level in the CB (zero pt. energy)
*     Ev1 = energy in eV of first quantum level in the VB (zero pt. energy)
*     Efc = Efco(1 - (pi**2/12)*(kT/Efco)**2) + Ec1 in eV @ T K
*     Efv = Efvo(1 - (pi**2/12)*(kT/Efvo)**2) + Ev1 in eV @ T K
```

```
      DO 10 K = 0,R
        GAM(K) = 0.0
        PHO(K) = INPh + K*S
        PH = PHO(K)
****  Summation over quantum numbers m and n performed
        DO 20 I = 1,M
              DO 30 J = 1,N
                GA = 0.0
                Evmn = CONv*((I/LY)**2 + (J/LZ)**2)
                Ermn = (CONc+CONv)*((I/LY)**2 + (J/LZ)**2)
             BR = PH - Ermn - Eg
             IF (BR.LT.0.0001) THEN
                GOTO 20
             ELSE
                BB = SQRT(BR) - 0.0001
****  Calculation of one-D Integral: Calling subroutine QGAUSS.
                 CALL QGAUSS(RINGD,AA,BB,GA)
             ENDIF
             GAM(K) = GAM(K) + GA
30           CONTINUE
20      CONTINUE
10    CONTINUE

      WRITE(5,6) 'PHO(K)-Eg'
7     FORMAT(1X,F10.7)
      DO 71 K = 0,R
      WRITE(5,7) PHO(K)-Eg
71    CONTINUE

****  GAMCON = Constant multiple of gain in units of 1.58511E10.
      WRITE(5,6) 'GAIN(K)'
      DO 72 K = 0,R
        GAMCON = LX*PHO(K)/(LY*LZ)
        GAMA(K) = GAMCON*GAM(K)
      WRITE(5,8) GAMA(K)
8     FORMAT(1X,E10.5)
72    CONTINUE

      WRITE(9,1) 'RUN PROGRAM AGAIN = 1/QUIT = any key'
      WRITE(9,1) 'CAUTION: PREVIOUS DATA WILL BE LOST !'
      READ*, ANSW
      IF (ANSW.EQ.1) THEN
      GO TO 100
      ELSE
      WRITE(9,1) 'GOODBYE !'
      GO TO 700
      ENDIF

700   END
```

```
**************************************************************************
      SUBROUTINE QGAUSS(FUN,A,B,SS)

*     This routine returns as SS the integral of the function FUN between limits A and B,
*     by ten-point Gaussian-Legendre integration: the function is evaluated exactly ten
*     times at interior points in the range of integration. X and W are the abscissas and
*     weights, resp.

      DIMENSION X(5),W(5)
      DATA X/.1488743389,.4333953941,.6794095682,.8650633666,
     &   .9739065285/
      DATA W/.2955242247,.2692667193,.2190863625,.1494513491,
     &   .0666713443/

      XM = 0.5*(B+A)
      XR = 0.5*(B-A)
      SS = 0.
*     This will be twice the average value of the function, since the
*     ten weights (5 numbers each used twice) sum to 2.
      DO 10 J=1,5
        DX = XR*X(J)
        SS = SS + W(J)*(FUN(XM+DX) + FUN(XM-DX))
10    CONTINUE
      SS = XR*SS
*     scale the answer to the range of integration.
      RETURN
      END

**************************************************************************
      FUNCTION RINGD(X)
*     Integrand of 1D no k-selection gain coefficient.

      COMMON/ATT/Eg,kT,Efc,Efv,Ermn,Evmn,PH
      REAL kT,Efc,Efv,Evmn,Ermn,PH,Fc,Fv,A,AX

      A = PH-Ermn-Eg
      AX = SQRT(A-X**2)
      Fc = EXP(-(Ph-Evmn-Eg-X**2-Efc)/kT)/
     &          (1+EXP(-(Ph-Evmn-Eg-X**2-Efc)/kT))
*     Fc and Fv are written thus, as a positive exponential power was
*     giving a numeric overflow during run-time.
      Fv = EXP(-(-Evmn-X**2+Efv)/kT)/
     &          (1+EXP(-(-Evmn-X**2+Efv)/kT))
      RINGD = (Fc - Fv)/AX
      RETURN
      END
**************************************************************************
```